Available online at www.sciencedirect.com

ScienceDirect

Geochimica et Cosmochimica Acta 166 (2015) 189–209

Geochimica et Cosmochimica Acta

www.elsevier.com/locate/gca

Assessing the impact of diagenesis on $\delta^{11}B$, $\delta^{13}C$, $\delta^{18}O$, Sr/Ca and B/Ca values in fossil planktic foraminiferal calcite

Kirsty M. Edgar [a,b,*], Eleni Anagnostou [c], Paul N. Pearson [a], Gavin L. Foster [c]

[a] School of Earth and Ocean Sciences, Cardiff University, Cardiff CF10 3AT, UK
[b] School of Earth Sciences, University of Bristol, Wills Memorial Building, Queens Road, Bristol BS8 1RJ, UK
[c] Ocean and Earth Science, University of Southampton, Southampton SO14 3ZH, UK

Received 27 November 2014; accepted in revised form 16 June 2015; Available online 24 June 2015

Abstract

The geochemical composition of foraminiferal tests is a valuable archive for the reconstruction of paleo-climatic, -oceanographic and -ecological changes. However, dissolution of biogenic calcite and precipitation of inorganic calcite (overgrowth and recrystallization) at the seafloor and in the sediment column can potentially alter the original geochemical composition of the foraminiferal test, biasing any resulting paleoenvironmental reconstruction. The $\delta^{11}B$ of planktic foraminiferal calcite is a promising ocean pH-proxy but the effect of diagenesis is still poorly known. Here we present new $\delta^{11}B$, $\delta^{13}C$, $\delta^{18}O$, Sr/Ca and B/Ca data from multiple species of planktic foraminifera from time-equivalent samples for two low latitude sites: clay-rich Tanzanian Drilling Project (TDP) Site 18 from the Indian Ocean containing well-preserved ('glassy') foraminifera and carbonate-rich Ocean Drilling Program (ODP) Site 865 from the central Pacific Ocean hosting recrystallized ('frosty') foraminifera. Our approach makes the assumption that environmental conditions were initially similar at both sites so most chemical differences are attributable to diagenesis. Planktic foraminiferal $\delta^{18}O$ and $\delta^{13}C$ records show offsets in both relative and absolute values between the two sites consistent with earlier findings that these isotopic ratios are strongly influenced by diagenetic alteration. Sr/Ca and B/Ca ratios in planktic foraminiferal calcite are also offset between the two sites but there is little change in the relative difference between surface and deep dwelling taxa. In contrast, $\delta^{11}B$ values indicate no large differences between well-preserved and recrystallized foraminifera suggesting that despite extensive diagenetic alteration the $\delta^{11}B$ of biogenic calcite appears robust, potentially indicative of a lack of free exchange of boron between pore fluids and the recrystallizing $CaCO_3$. Our finding may remove one potential source of uncertainty in $\delta^{11}B$ based pH reconstructions and provide us with greater confidence in our ability to reconstruct pH in the ancient oceans from at least some recrystallized foraminiferal calcite. However, further investigations should extend this approach to test the robustness of our findings across a range of taphonomies, ages and burial settings.

1. INTRODUCTION

Foraminifera precipitate their calcium carbonate tests from the seawater in which they live, providing a record of key environmental conditions at the time and depth of calcification (e.g., Lea, 2014). There are many chemical proxies (elemental and isotopic) that can be measured in foraminiferal tests to reconstruct both past environments and organism ecology. To highlight a few, the classic $\delta^{18}O$ and $\delta^{13}C$ proxies provide insights into changes in past ocean temperatures, salinity and/or global ice volume, and ocean dissolved inorganic carbon, respectively (Lea, 2014; Zeebe and Wolf-Gladrow, 2001). Sr/Ca ratios are more

* Corresponding author at: School of Earth Sciences, University of Bristol, Wills Memorial Building, Queens Road, Bristol BS8 1RJ, UK. Tel.: +44 (0) 117 331 5211.
E-mail address: kirsty.edgar@bristol.ac.uk (K.M. Edgar).

http://dx.doi.org/10.1016/j.gca.2015.06.018
0016-7037/

difficult to interpret reflecting some combination of calcification temperature, calcification rate, carbonate chemistry, seawater Sr/Ca, salinity and/or dissolution (e.g., Brown and Elderfield, 1996; Lea et al., 1999; Stoll et al., 1999) but may be a good qualitative indicator of post-mortem alteration of foraminiferal calcite (Baker et al., 1982; Bralower et al., 1997; Regenberg et al., 2007).

The most powerful tool that we have to reconstruct paleo-ocean pH and ultimately past concentrations of atmospheric CO_2 is the boron isotopic composition (expressed as $\delta^{11}B$) of planktic foraminifera (Foster, 2008; Foster et al., 2012; Hemming and Hönisch, 2007; Hönisch et al., 2009; Palmer et al., 1998; Pearson and Palmer, 1999, 2000; Penman et al., 2014; Spivack et al., 1993). The B/Ca of planktic foraminiferal tests also looked to be a promising candidate for reconstructing surface ocean pH (Yu et al., 2007b) or $[CO_3]^{2-}$ (Foster, 2008). However, subsequent investigations indicate that the controls on B/Ca are not clear and thus, interpretation of B/Ca records (particularly in the geological record) may not be as straightforward as originally anticipated (Allen and Hönisch, 2012; Allen et al., 2012; Babila et al., 2014; Henehan et al., 2015).

There is increasing awareness of how both the microstructure and geochemistry (elemental and isotopic) of fossil foraminifera tests from deep-sea sediments are modified by post-mortem diagenetic alteration (Norris and Wilson, 1998; Pearson and Burgess, 2008; Pearson et al., 2001, 2007; Schrag et al., 1995; Sexton et al., 2006a; Wilson et al., 2002). Yet, the impact of diagenesis on foraminiferal calcite, in particular on new proxies such as $\delta^{11}B$ and B/Ca, is not well known and thus represents a potentially large source of uncertainty in paleo-reconstructions of ocean carbonate chemistry.

1.1. Impact of diagenesis on the microstructure and geochemistry of foraminiferal tests

There are at least three distinct diagenetic processes by which foraminiferal test wall structure and morphology can be modified: partial dissolution, overgrowth and recrystallization. All three can potentially act to offset the original geochemistry of foraminiferal tests post-mortem either in the water column or at and beneath the seafloor (Pearson and Burgess, 2008). Firstly, calcite dissolution can modify the elemental and isotopic composition of foraminiferal calcite (e.g., Brown and Elderfield, 1996; Coadic et al., 2013; Lohmann, 1995; Pearson, 2012). For instance, one hypothesis suggests that ontogenetic calcite is more susceptible to dissolution than gametogenic calcite precipitated at greater depths and as such with a potentially different chemical composition (Bé et al., 1975; Hemleben et al., 1989). Secondly, precipitation of inorganic calcite from sediment pore fluids onto the internal and/or external walls of foraminiferal tests (overgrowths) can add significant amounts of secondary calcite to the test which may be geochemically very different to the primary test composition. These inorganic calcite crystals are typically much larger than their biogenic counterparts making them easy to identify by scanning electron microscopy and can, in some cases, completely infill specimens (Pearson and Burgess, 2008). Finally, the *in-situ* replacement of the original microgranular calcite test wall structure by larger, blockier calcite crystals (Pearson and Burgess, 2008; Pearson et al., 2001; Sexton et al., 2006a) is frequently termed either *neomorphism* (as per Folk, 1965) or *recrystallization* (Sorby, 1879). These two terms are sometimes used interchangeably because of their overlapping definitions. However, neomorphism encompasses all *in-situ* transformations of older crystals to new crystals of the same mineral or its polymorph (recrystallization and inversion, respectively) (Folk, 1965). This term is most commonly applied to the aragonite–calcite transformation or when the original mineral phase is unknown. Here we use the term recrystallization which explicitly refers to the replacement of primary crystals by new crystals of the same mineral species, in this case calcite (see Folk, 1965 for discussion). Recrystallization is potentially gradual and very localized such that the new crystal lattice can be constructed wholly or in part from ions in the pre-existing crystal phases. There may be many rounds of dissolution and re-precipitation as a new crystal is formed (Pearson and Burgess, 2008) leading to foraminifera appearing opaque or 'frosty' under reflected light (Sexton et al., 2006a).

The potential for diagenetic effects on the isotopic composition of marine carbonates to complicate paleoclimatic reconstructions is best illustrated by the so-called 'cool-tropic paradox' (D'Hondt and Arthur, 1996). This is the mismatch between climate simulations indicating warming at all latitudes and Cretaceous and Early Paleogene paleo-data that reflect similar to modern or cooler than modern sea surface temperatures (SSTs) (D'Hondt and Arthur, 1996). This discrepancy arises from analysis of foraminifera that yield artificially high $\delta^{18}O$ values and thus, underestimates of tropical SSTs because of diagenetic alteration of tropical planktic foraminiferal calcite at the seafloor. One solution to the 'cool-tropic' paradox has been to target sites containing well-preserved foraminifera obtained from clay-rich sediments (e.g., Pearson et al., 2001). These foraminifera typically show little evidence of micron-scale diagenetic alteration appearing translucent under the binocular light microscope or 'glassy' and contain near-pristine biogenic calcite (e.g., Burgess et al., 2008; Norris and Wilson, 1998; Pearson et al., 2001, 2007; Sexton et al., 2006a; Wilson and Norris, 2001; Wilson et al., 2002). The relatively impermeable nature of these clay-rich sediments may prevent significant interaction of foraminiferal calcite with surrounding pore fluids leading to excellent carbonate preservation (Bown et al., 2008). However, sites containing glassy foraminifera are relatively rare (and largely undersampled) in the geological record and are usually limited to continental shelves and slopes. The majority of available deep-sea sites for paleoceanographic reconstructions are carbonate-rich and predominantly contain recrystallized foraminiferal calcite (see Schrag et al., 1995). Despite an obvious diagenetic impact on several well-known geochemical proxies including $\delta^{18}O$, some component of the original chemical composition is often retained (e.g., Kozdon et al., 2011; Pearson et al., 2001; Sexton et al., 2006a). Hence, the identification

and quantification of diagenetic alteration and its impact on the chemical composition of fossil foraminiferal calcite remains a major challenge for paleoenvironmental reconstructions.

The use of $\delta^{11}B$ in marine carbonates as a paleo-pH proxy has undergone a revival in recent years in-line with the increased focus on understanding past changes in ocean acidification and the link between atmospheric CO_2 and climate (Badger et al., 2013; Foster et al., 2012; Hönisch et al., 2009; Pearson et al., 2009; Penman et al., 2014). Early studies suggest that diagenesis could modify the $\delta^{11}B$ of bulk carbonate sediments (Spivack and You, 1997), but more recent work suggests that the $\delta^{11}B$ of foraminiferal tests may be more robust. Specifically, as with $\delta^{18}O$ and $\delta^{13}C$ records (e.g., Pearson et al., 2001), diagenesis does not apparently overprint inter-specific differences in the $\delta^{11}B$ of fossil foraminiferal calcite (Foster et al., 2012; Palmer et al., 1998; Pearson and Palmer, 1999). Furthermore, there is close agreement between time-equivalent planktic foraminiferal $\delta^{11}B$ values measured in Mid-Miocene aged *Globigerinoides sacculifer* at ODP Sites 926 and 761, and in the clay-rich Ras-il Pellegrin section in Malta, all three of which have different burial histories and carbonate preservation (Badger et al., 2013; Foster et al., 2012). Similarly, recently published planktic foraminiferal $\delta^{11}B$ data from a suite of deep-sea sites spanning the Paleocene–Eocene Thermal Maximum record similar patterns of change across the event implying minimal diagenetic bias of the $\delta^{11}B$ values given the different preservation histories of the analysed sites (Penman et al., 2014). In contrast, partial dissolution of planktic foraminifera has been hypothesised to explain lower than expected $\delta^{11}B$ values for some species reported from sites situated at greater water depths (Hönisch and Hemming, 2004; Ni et al., 2007; Seki et al., 2010).

To assess the impact of diagenetic alteration on planktic foraminiferal calcite we present a suite of new $\delta^{11}B$, $\delta^{13}C$, $\delta^{18}O$, B/Ca and Sr/Ca data in planktic foraminiferal species from two time-equivalent sedimentary settings with different taphonomies. Foraminiferal tests from ODP Site 865 are recrystallized whereas those at Tanzanian Drilling Project (TDP) Site 18 have experienced little or no recrystallization. Nearly identical middle Eocene planktic foraminiferal assemblages are found at these two tropical sites implying very similar ages and paleoenvironmental conditions. Further similar oceanographic settings (and temperatures) are inferred for the two sites from Eocene General Circulation Model (GCM) simulations (Huber and Caballero, 2011; Tindall et al., 2010). Thus, our basic assumption is that the elemental and isotopic composition of the various species and their size fractions were originally similar at both sites, hence any large and consistent differences that we observe are likely to be the result of differential diagenesis. At each of the sites we analysed morphospecies that calcified across a substantial environmental gradient in temperature, $\delta^{13}C$, pH etc., from the surface mixed layer through to the deep-thermocline. More specifically, we assess: (1) the consistency of relative depth rankings of planktic foraminifera in the water column at each site; (2) any inter-specific offsets; (3) differences in the absolute values measured at the two sites; (4) the susceptibility of different taxa to diagenetic alteration; and (5) potential explanations for the chemical trends observed.

2. MATERIALS AND METHODS

2.1. Site location

This study utilises sediments from TDP Site 18, a short core (28.4 m long) drilled in the Eocene Masoko Formation (9°261.982′S, 39°53.389′E; Fig. 1) which comprises greenish-grey silty clays inter-bedded with occasional limestone debris flows (Nicholas et al., 2006). The entire core falls within short-lived planktic foraminiferal Zone E12 defined by the total range of the planktic foraminifera *Orbulinoides beckmanni* (~40.0–40.5 Ma; Nicholas et al., 2006; Wade et al., 2011). Samples utilised here are from dark greenish-grey silty clays situated in the lowermost part of the core below the weathering oxidation front. Foraminifer assemblages confirm that the studied sediments belong to the lower part of Biozone E12, prior to the warming associated with the Middle Eocene Climate Optimum (MECO). Sediments were deposited on the mid or outer shelf-upper continental slope under estimated paleowater depths of >300 m based on *in-situ* benthic foraminiferal assemblages (Nicholas et al., 2006). Seismic, sedimentary facies, paleogeography, and nannofossil and planktic foraminiferal assemblages indicate that these sediments were deposited under open-ocean conditions with waters derived from the Indian Ocean subtropical gyre (Bown et al., 2008; Pearson et al., 2007).

Ocean Drilling Program Hole 865C (18°26.425′N, 179°33.339′W; 1300–1500 m paleowater depth) is located on the summit of Allison Guyot under the North Pacific oligotrophic gyre in the western Pacific Ocean (Fig. 1; Shipboard Scientific Party, 1993). Eocene sediments are predominantly foraminiferal nannofossil ooze and foraminiferal sands and are shallowly buried (<100 m). Samples here are from uppermost planktic foraminiferal Zone E11/lowermost Zone E12 as rare transitional specimens between *Globigerinatheka euganea* and *O. beckmanni* are present but also *Acarinina bullbrooki*, ~40.5 Ma (age assignment based on Wade et al., 2011). Samples were taken from this transitional interval because no stable

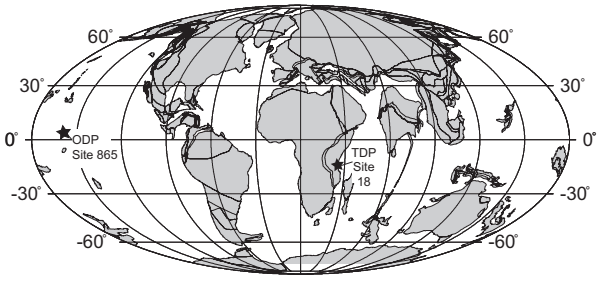

Fig. 1. Eocene paleogeographic reconstruction for ~40 Ma showing the paleoposition of study sites: ODP Site 865 (Bralower et al., 1995) and TDP Site 18 (black stars). Base map generated from www.odsn.de.

isotope stratigraphy is currently available for ODP Site 865 and we wanted to ensure that we did not take samples from the MECO, which could bias our comparison.

2.2. Sample material

Sediment samples were initially disaggregated in de-ionised water for ten minutes prior to washing over a 63 μm sieve and then dried at 50 °C overnight. To obtain sufficient foraminifera for all analyses and to minimise any offsets resulting from comparison of potentially disparate timeslices, 6–12 cm of core material was combined for analysis at each site (equivalent to ~6–15 kyrs). Data from ODP Site 865 are from Samples 865C-5H-5, 113–116 and 107–110 cm (38.89 and 38.95 mbsf, respectively) and for TDP from Samples 18–18–2, 44–54, 62–70 and 78–81 cm (27.19, 27.36 and 27.50 m, respectively). To further minimise any inter-specific, ontogenetic and metabolic effects on isotopic and elemental values we picked mono-specific foraminiferal separates and wherever possible from a narrow sieve size range (~50 μm window). Each mono-specific separate comprised ~3–4 mg of material equivalent to ~200 individuals in the 250–300 μm sieve size fraction. Planktic foraminiferal species were identified following the taxonomic criteria of Pearson et al. (2006).

To constrain bottom water conditions at each of the sites the epifaunal benthic foraminifera *Cibicidoides* was also measured (0.7–1.0 mg or ~6 individuals). It is important to note that benthic foraminiferal chemical values at the two sites are not necessarily comparable with one another because our TDP and ODP samples reflect bottom water conditions on the continental slope and from mid-bathyal water depths, respectively.

2.3. Scanning electron and light microscopy

To document the extent of diagenetic alteration of fossil planktic foraminiferal tests, representative specimens from each site were selected for imaging. Reflected light microscope images were captured using a Leica DFC 480 camera and Qimaging software – samples were immersed in water before imaging. Prior to mounting, all specimens were ultrasonicated in de-ionised water for approximately two seconds to remove any loosely adhered material from the test surface. Individual tests and broken specimens were then mounted on a black adhesive tab on top of a metal SEM stub. Samples were gold sputter-coated for SEM analysis on a Veeco FEI (Phillips) XL30 environmental SEM at the School of Earth and Ocean Sciences at Cardiff University.

2.4. Stable isotope and elemental analyses

Paired isotopic ($\delta^{18}O$, $\delta^{13}C$ and $\delta^{11}B$) and elemental analyses were conducted on each mono-specific foraminiferal separate. Specimens in each separate were crushed, homogenised and then divided into two parts with the majority analysed for $\delta^{11}B$ and trace metals (~97%) and ~100 μg reserved for $\delta^{18}O$ and $\delta^{13}C$ analyses.

All $\delta^{13}C$ and $\delta^{18}O$ measurements were made on a Thermo Scientific Delta V Advantage mass spectrometer coupled to a GasBench II in the School of Earth and Ocean Sciences at Cardiff University and are reported relative to the Vienna Pee Dee Belemnite (VPDB) standard. Stable isotope values have a standard external analytical precision of 0.06‰ for $\delta^{13}C$ and 0.07‰ for $\delta^{18}O$ (at 68% confidence). Mono-specific separates were cleaned for elemental and $\delta^{11}B$ analysis following the oxidative cleaning methodology of Barker et al. (2003). The reductive step designed to remove metal oxide coatings was omitted because these coatings are not a major source of boron contamination (the main focus of this study; Yu et al., 2007a) and the reducing reagent is corrosive causing partial dissolution of foraminiferal carbonate and artificial lowering key element/Ca ratios (Barker et al., 2003). Thus, we do not present any new Mg/Ca data here because Fe–Mn oxide coatings (with high [Mg]) are present on samples from TDP Site 18 but not on those from ODP Site 865 rendering a direct comparison of Mg/Ca ratios from these two sites invalid. Consistent with Yu et al. (2007a) we find no correlation between B/Ca and indicators of Fe–Mn oxide coatings indicating that [B] is low or absent in Fe–Mn oxide coatings. Following cleaning but prior to $\delta^{11}B$ analysis a small aliquot (~7%) of each dissolved foraminiferal separate was analysed for minor and trace elements on a Thermo Element 2 Inductively Coupled Plasma Mass Spectrometer (ICP-MS) at the University of Southampton to test the efficiency of the oxidative cleaning protocol and determine the concentration of boron and strontium in each foraminiferal separate. Subsequently boron was separated from dissolved foraminiferal separates using amberlite IRA-743, a boron-specific anion exchange resin, following the method of Foster (2008). $\delta^{11}B$ analyses were then conducted on a Thermo Scientific Neptune Multi-Collector ICP-MS at the University of Southampton and are reported relative to the NIST-SRM 951 boric acid standard (Catanzaro et al., 1970). External precision is described by the reproducibility of repeat analyses of Japanese Geological Survey *Porites* coral standard (JCP; $\delta^{11}B = 24.3‰$) and is dependent on the amount of boron analysed (Rae et al., 2011). In a slight departure from Henehan et al. (2013) we use two equations, one for single analyses and one for duplicate analyses (Eqs. (1) and (2), respectively) to determine external precision on each species separate.

$$2\sigma = 6.82 * \exp(-32.61 * [^{11}B]) + 0.285 * \exp(-0.183 * [^{11}B]) \quad (1)$$

$$2\sigma = 2.25 * \exp(-23.0 * [^{11}B]) + 0.278 * \exp(-0.639 * [^{11}B]) \quad (2)$$

where $[^{11}B]$ is the ^{11}B signal in Volts.

2.5. Constraining the composition and fraction of inorganic calcite contributing to foraminiferal test chemistry

To quantify the amount of chemical alteration that has occurred in frosty specimens, which may be independent of how texturally recrystallized specimens are, we define an 'Index of $\delta^{18}O$ diagenetic overprint'. We developed species-specific linear regressions between the $\delta^{18}O$ values

of 'primary' foraminiferal calcite and inorganic calcite precipitated at the seafloor assuming contributions of 0 and 100%, respectively to foraminiferal test chemistry. The $\delta^{18}O$ of inorganic calcite is based on the $\delta^{18}O$ of epifaunal benthic *Cibicidoides* sp. measured at ODP Site 865 (0.85‰) which is thought to precipitate its test in isotopic equilibrium with bottom waters (Bemis et al., 1998). We assume that the $\delta^{18}O$ of primary calcite is equivalent to glassy species-specific $\delta^{18}O$ values (Table 1).

Using the calculated Index of $\delta^{18}O$ diagenetic overprint, mass balance equations (Eqs. (3) and (4)) were solved to estimate the B/Ca and $\delta^{11}B$ of inorganic calcite.

$$B/Ca_G * F_G + B/Ca_I * F_I = B/Ca_F * 1 \quad (3)$$

$$\delta^{11}B_G * B/Ca_G * F_G + \delta^{11}B_I * B/Ca_I * F_I = \delta^{11}B_F * B/Ca_F * 1 \quad (4)$$

Subscript letters in Eqs. (3) and (4) refer to the isotopic value/elemental ratio in 'glassy' calcite ($_G$), inorganic calcite ($_I$) and in 'frosty' calcite ($_F$). F_I is the fraction of the total test chemistry that is attributed to inorganic calcite approximated by the Index of $\delta^{18}O$ diagenetic overprint and (F_G) is the remaining fraction of test chemistry attributed to primary calcite calculated by:

$$F_G = (100 - F_I)/100 \quad (5)$$

2.6. Hydrographic and pore fluid data

To investigate the $\delta^{11}B$ value of inorganic calcite precipitated from the water column and sediment pore fluids we calculate the $\delta^{11}B$ of $B(OH)_4^-$ at ODP Site 865 (no pore fluid data are available for TDP Site 18). Hydrographic data is taken from World Ocean Circulation Experiment section P14N (Sites 88 and 91) located close to ODP Site 865 today (Roden et al., 1995). The $\delta^{11}B$ of $B(OH)_4^-$ in sediment pore fluids ($\delta^{11}B_{BOH_4\text{-pore fluid}}$) was determined using chemical data from ODP Site 865 collected by the Shipboard Scientific Party (1993). Profiles were calculated in CO2sys (van Heuven et al., 2011) using salinity, temperature, depth, alkalinity, pH, and the concentrations of silicate and phosphate from each site. Total B (B_T) was estimated from salinity to give the K_B. B_T and K_B were then used to calculate the amount of BOH_3 and $B(OH)_4^-$ in the water column and pore fluids assuming a modern $\delta^{11}B_{sw} = 39.61‰$ (Foster et al., 2010). The boron isotopic fractionation factor of 1.0272 was applied throughout (Klochko et al., 2006) and phosphate was set at 2 μmol/kg. Sparse *in-situ* down-hole temperature data was available for ODP Site 865 thus, a geothermal gradient of 46 °C/km from nearby sites was used to calculate the temperature for each of the sample depths (Sager et al., 1993). The temperature gradient has little impact on calculated $\delta^{11}B$ values.

3. RESULTS

3.1. Middle Eocene planktic foraminiferal taphonomy

Planktic foraminifera from TDP Site 18 are glassy *sensu* Sexton et al. (2006a) (Fig. 2a–c) akin to non-encrusting foraminiferal taxa collected live from the modern ocean. SEM images reveals that the test walls of these planktic foraminiferal are constructed from aggregates of sub-micron scale crystallites (microgranules sensu Blow, 1979) creating smooth interior and exterior surfaces with fine scale surface features such as spines, pores and carbonate pustules (also known as 'muricae') preserved (Fig. 2d–i). In cross section, the test wall is cohesive with biogenic layers and no apparent gaps. In contrast, planktic foraminifera from ODP Site 865 are opaque ('frosty') under reflected light indicating that the walls have been recrystallized (Fig. 2j–l). SEM analysis shows that external test surfaces are overgrown by relatively large (>1 μm), loosely packed calcite crystals that act to obscure the pores and other surface ornamentation. The delicate biogenic muricae that are characteristic of the dominant Eocene surface dwelling groups *Acarinina* and *Morozovelloides* have been overgrown by large, euhedral, blade-like crystals presumably having acted as a locus for crystallisation (Fig. 2g vs. o). In cross-section it is evident that the structural integrity of the test wall has been compromised with dissolution exploiting existing lines of weakness such as the position of the former primary organic membrane leading to delamination of the inner test wall and there are pervasive small inorganic crystals projecting from the internal test surface (see also Pearson et al., 2007, 2015; Sexton et al., 2006a for similar comparisons). However, specimens at both sites are free of significant infilling. Notably the average test weight of frosty specimens is ~30% lower than in their glassy counterparts reflecting the loss of material by dissolution and subsequent looser packing of inorganically precipitated crystals within the recrystallized test walls (Table 2).

3.2. Foraminiferal geochemical data

3.2.1. Foraminiferal $\delta^{18}O$ and $\delta^{13}C$ and species ecology

The main geochemical tools used to reconstruct the paleoecology of fossil foraminifera, e.g., water depth habitat and presence/absence of algal photosymbionts, are the carbon and oxygen isotopic ($\delta^{13}C$ and $\delta^{18}O$) compositions of foraminiferal tests (Berger et al., 1978; Birch et al., 2013; Fairbanks et al., 1980; Pearson, 2012; Spero and Williams, 1988). Their utility arises because ^{12}C is preferentially utilised by photosymbionts and phytoplankton, leaving the foraminiferal microenvironment and ambient seawater enriched in ^{13}C. Below the photic zone, the ^{12}C of the water column increases relative to surface waters as a function of reduced photosynthetic activity and remineralisation of ^{12}C enriched-organic matter leading to lower test $\delta^{13}C$ values (many foraminifera also lack photosymbionts). In contrast, foraminiferal test $\delta^{18}O$ values increase with depth because of the decrease in temperature and the strong temperature-dependence of oxygen isotope fractionation between ambient seawater and foraminiferal calcite during calcification (Bemis et al., 1998; Emiliani, 1954; Pearson, 2012). Thus, taxa that precipitate their tests in warm surface waters have relatively low $\delta^{18}O$ and high $\delta^{13}C$ values relative to those that occupy a deeper position in the water column (Berger et al., 1978; Birch et al., 2013; Fairbanks et al., 1980; Pearson, 2012; Spero and Williams, 1988).

Table 1
$\delta^{18}O$ and $\delta^{13}C$ values for glassy and frosty foraminifera from TDP Site 18 and ODP Site 865, respectively.

Species	Depth habitat	Sieve size fraction (μm)	TDP Site 18 $\delta^{18}O$ (‰, VPDB)	Paleotemperature (°C)	TDP Site 18 $\delta^{13}C$ (‰, VPDB)	ODP Site 865 $\delta^{18}O$ (‰, VPDB)	Paleotemperature (°C)	ODP Site 865 $\delta^{13}C$ (‰, VPDB)	$\Delta\delta^{18}O$* (‰, VPDB)	$\Delta\delta^{13}C$* (‰, VPDB)
Morozovelloides coronatus	Mixed layer	250–300	−2.94	29.3	2.68	−0.47	16.8	3.07	2.48	0.39
Morozovelloides crassatus	Mixed layer	250–300	−3.09	30.1	2.97	−0.40	16.6	2.94	2.69	−0.03
Morozovelloides lehneri	Mixed layer	212–250	−3.43	31.8	2.81	−0.23	15.7	2.80	3.20	−0.01
Acarinina mcgowrani	Mixed layer	212–250	−3.13	30.3	2.41	−0.71	18.0	2.87	2.42	0.46
Acarinina praetopilensis	Mixed layer	250–300	−3.13	30.3	3.23	−0.52	17.1	3.14	2.60	−0.10
Acarinina rohri	Mixed layer	250–300	−3.14	30.3	3.36	−0.63	17.6	3.07	2.50	−0.29
Acarinina topilensis	Mixed layer	250–300	−3.09	30.1	3.44	−0.53	17.2	3.17	2.56	−0.27
Subbotina senni	Mixed layer encrusted	250–300	−3.06	29.9	1.90	−1.07	19.7	2.31	1.98	0.40
Globigerinatheka euganea	Mixed layer encrusted	>500	−2.80	28.6	2.47	−1.05	19.6	2.97	1.75	0.49
Turborotalia cerroazulensis	Intermediate	250–300	−2.87	28.9	0.83	−0.13	15.3	1.70	2.75	0.87
Turborotalia pomeroli	Intermediate	250–300	−2.55	27.3	0.78	−0.03	14.8	1.67	2.52	0.89
Subbotina corpulenta	Thermocline	250–425	−2.13	25.2	0.86	0.48	12.5	1.67	2.61	0.81
Subbotina crociapertura	Thermocline	300–355	−2.46	26.8	0.98	−0.25	15.8	1.85	2.21	0.88
Cibicidoides sp.	Seafloor	250–300	−1.44	17.8	0.73	–	–	–	–	–
Cibicidoides havanensis	Seafloor	355–425	–	–	–	0.85	7.5	0.66	–	–

Paleotemperatures calculated using the equation of Kim and O'Neil (1997) reformulated by Bemis et al. (1998) with corrections for ice volume (0.8‰; Cramer et al., 2011) and paleolatitude (0.76‰ for ODP Site 865 and 0.83‰ for TDP Site 18 following Zachos et al. (1994)) applied.
Cibicidoides are assumed to have precipitated their test in oxygen isotopic equilibrium with ambient seawater following Bemis et al. (1998)
* Difference in stable isotope values in each species at ODP Site 865 and TDP Site 18.

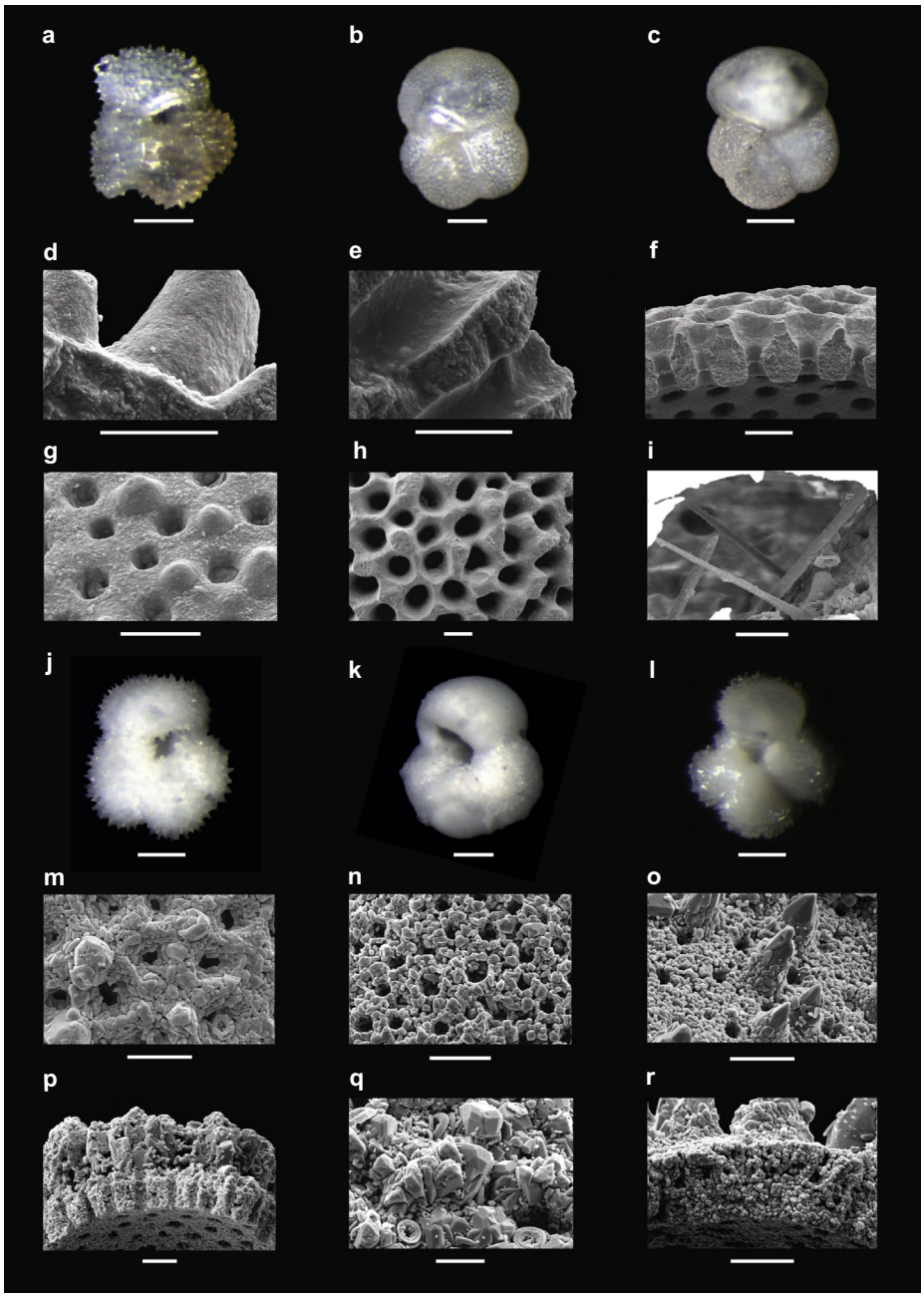

Fig. 2. Reflected light and scanning electron micrographs (RLM and SEM) of planktic foraminifera contrasting well preserved (a–i) and poorly preserved (j–r) wall textures. RLM of glassy textures. (a) Sample TDP Site 18 18–2, 44–54 cm *Acarinina praetopilensis*; (b) Sample TDP Site 18 18–2, 44–54 cm *Turborotalia pomeroli*; (c) Sample TDP Site 18 18–2, 44–54 cm *T. pomeroli*. SEM of glassy foraminifera wall textures. (d) Sample TDP Site 18 18–2, 62–70 cm, close-up of muricae in *A. topilensis*; (e) Sample TDP Site 18 18–2, 62–70 cm, wall cross-section of *Globigerinatheka* sp.; (f) Sample TDP Site 18 18–2, 44–54 cm, wall cross-section of *Subbotina linaperta*; (g) Sample TDP Site 18 18–2, 44–54 cm, exterior test surface of *T. cerroazulensis*; (h) Sample TDP Site 18 18–2, 44–54 cm, exterior test surface of *S. eocaena*; (i) Sample TDP Site 18 18–2, 44–54 cm, delicate calcite spines preserved inside aperture of *G. euganea* (white area is charging on specimen). RLM of frosty specimens. (j) Sample ODP Site 865C 15–5, 107–110 cm *A. praetopilensis*; (k) Sample ODP Site 865C 15–5, 107–110 cm *T. pomeroli*; (l) Sample ODP Site 865C 15–5, 107–110 cm *Morozovelloides crassatus*. SEMs of frosty wall textures. (m) Sample ODP Site 865C 15–5, 107–110 cm, exterior test wall of *S. senni*; (n) Sample ODP Site 865C 15–5, 107–110 cm, exterior test wall of *M. lehneri*; (o) Sample ODP Site 865C 15–5, 107–110 cm, exterior test wall of *M. crassatus*; (p) Sample ODP Site 865C 15–5, 107–110 cm, wall cross-section in *T. pomeroli*; (q) Sample ODP Site 865C 15–5, 107–110 cm, wall cross-section of *Globigerinatheka* sp.; (r) Sample ODP Site 865C 15–5, 107–110 cm, wall cross-section of *A. mcgowrani*. All scales bars are 100 μm for whole specimens and 10 μm for wall texture images.

Table 2
Sr/Ca and B/Ca values, and test weights for glassy and frosty foraminifera from TDP Site 18 and ODP Site 865, respectively.

Species	TDP Site 18 Sr/Ca (mmol/mol)	ODP Site 865 Sr/Ca (mmol/mol)	Sr/Ca offset (mmol/mol)	% of 'primary' Sr/Ca lost*	TDP Site 18 B/Ca (μmol/mol)	ODP Site 865 B/Ca (μmol/mol)	B/Ca offset (μmol/mol)	% of 'primary' B/Ca lost*	TDP Site 18 average test weight (μg)	ODP Site 865 average test weight (μg)
Morozovelloides coronatus	1.44	0.88	0.56	39.1	72.89	56.88	16.01	22.0	15.9	9.9
Morozovelloides crassatus	1.43	0.81	0.62	43.2	69.63	51.27	18.36	26.4	14.3	11.0
Morozovelloides crassatus	1.43	0.83	0.59	41.4	69.65	51.14	18.51	26.6	–	–
Morozovelloides lehneri	1.45	0.86	0.59	40.8	74.71	57.66	17.05	22.8	14.3	8.4
Acarinina mcgowrani	1.38	0.90	0.47	34.4	62.67	53.84	8.83	14.1	10.6	8.0
Acarinina praetopilensis	1.37	0.89	0.48	35.1	62.88	56.65	6.22	9.9	20.3	10.8
Acarinina rohri	1.29	0.90	0.39	30.0	62.22	56.85	5.37	8.6	20.2	13.0
Acarinina topilensis	1.53	0.90	0.63	41.2	70.50	60.60	9.90	14.0	16.1	11.1
Subbotina senni	1.45	1.11	0.34	23.4	68.02	57.59	10.43	15.3	20.7	17.6
Globigerinatheka euganea	1.32	1.10	0.22	16.3	44.79	41.74	3.05	6.8	102.5	76.0
Turborotalia cerroazulensis	1.56	1.00	0.56	35.8	54.60	36.74	17.86	32.7	20.8	17.0
Turborotalia pomeroli	1.56	1.00	0.57	36.4	52.81	34.45	18.36	34.8	20.3	13.9
Subbotina corpulenta	1.56	1.07	0.49	31.3	40.76	30.92	9.84	24.1	–	–
Subbotina crociapertura	1.50	0.98	0.53	35.2	45.43	33.37	12.06	26.6	32.9	25.8
Cibicidoides spp^	1.30	1.06	–	–	157.23	112.02	–	–	–	–

Long term precision of standards gives an uncertainty of 2% for Sr/Ca and 5% for B/Ca ratios.
* % loss of X/Ca from samples = Glassy or 'primary' TDP Site 18 Sr/Ca – Frosty ODP Site 865 Sr/Ca ratios.
^ *Cibicidoides* data are not directly comparable with one another because of different water depths of two sites.

Here we show $\delta^{18}O$ and $\delta^{13}C$ cross-plots (Table 1; Fig. 3a and b), for all of the species analysed at each of the study sites. Well-preserved specimens from TDP Site 18 indicate species ecologies consistent with previous findings (e.g., Edgar et al., 2013a; John et al., 2013; Pearson et al., 1993, 2001; Sexton et al., 2006b; Wade et al., 2008). Specifically, the muricate taxa *Morozovelloides* and *Acarinina* have among the lowest $\delta^{18}O$ and highest $\delta^{13}C$ values in the assemblage suggesting that they lived in the uppermost water column and were likely host to dinoflagellate photosymbionts. *G. euganea* and *Subbotina senni* have a similar surface dwelling habitat to the muricate taxa but develop a thick calcite crust in deeper waters towards the end of their life. The lower $\delta^{13}C$ values of *S. senni* than *G. euganea* (Fig. 3a and b) is likely attributable to ontogenetic effects resulting from the large difference in the size fractions measured between the two species (250–300 μm versus >500 μm, respectively; Edgar et al., 2013a) and/or the absence of photosymbionts. *Turborotalia* and *Subbotina* (other than *S. senni*) have isotopic compositions suggesting calcification at greater depths in the upper and lower thermocline, respectively and asymbiotic ecology. Finally, the epifaunal benthic *Cibicidoides* spp. record the highest $\delta^{18}O$ and lowest $\delta^{13}C$ values in the foraminiferal assemblage. Species isotope data show a similar overall pattern at the two study sites with two notable exceptions – in contrast to observations from TDP Site 18, *G. euganea* and *S. senni* at ODP Site 865 have the lowest $\delta^{18}O$ values in the assemblage (Fig. 3a vs. b).

$\delta^{18}O$ values in the same species (and size fraction) are consistently higher in recrystallized planktic foraminifera from ODP Site 865 than in glassy foraminifera from TDP

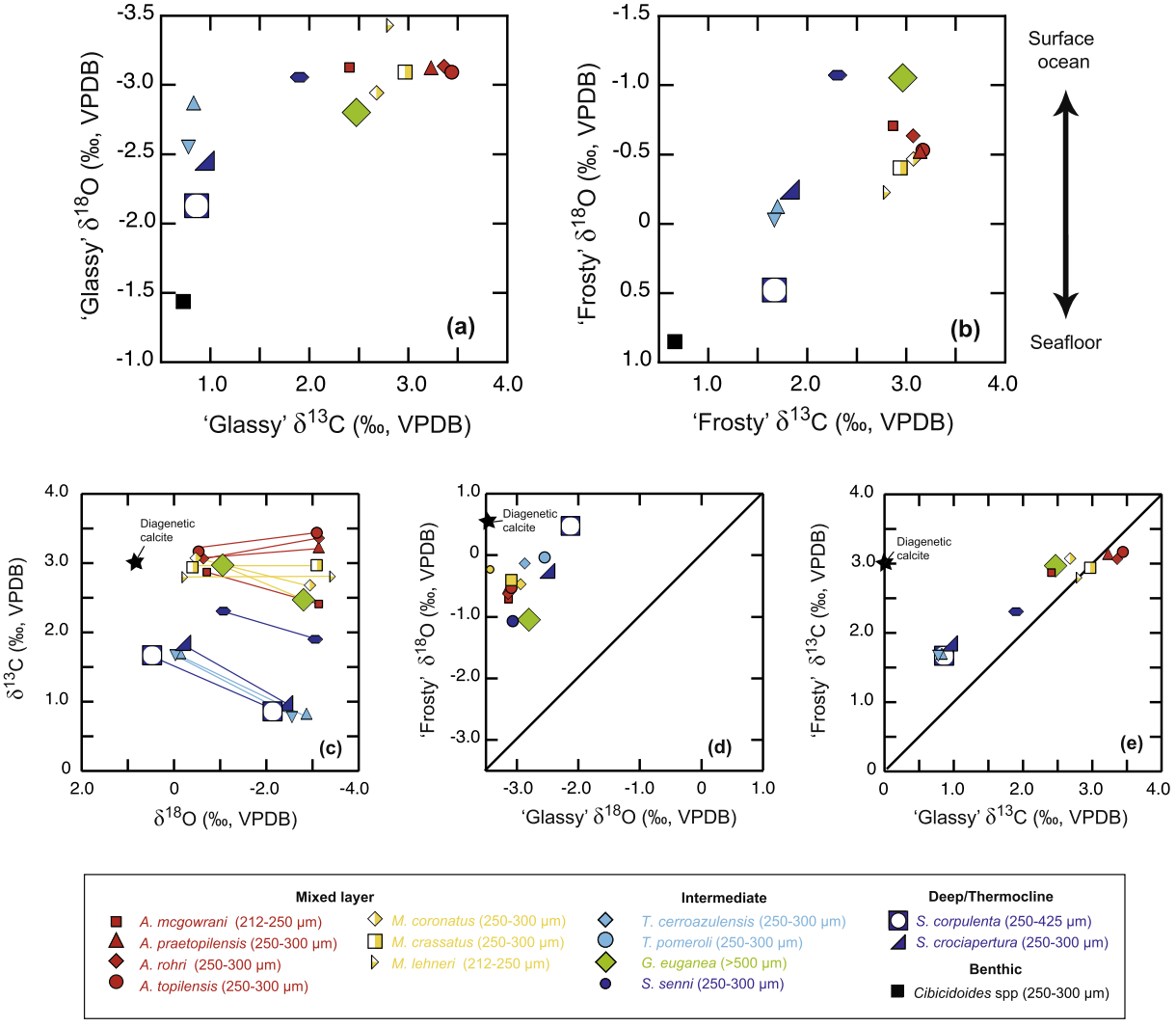

Fig. 3. Middle Eocene multi-species stable isotope ($\delta^{18}O$ versus $\delta^{13}C$) arrays for glassy (a) and frosty (b) foraminiferal samples from TDP Site 18 and ODP Site 865, respectively. Vertical arrows to the right of panel (b) = species ecology. (c) Comparison of frosty vs. glassy $\delta^{18}O$ and $\delta^{13}C$ highlighting larger $\delta^{18}O$ versus $\delta^{13}C$ offsets in absolute values. Comparison of $\delta^{18}O$ (d) and $\delta^{13}C$ (e) arrays at the two sites relative to a 1:1 relationship (diagonal line). Inorganic/diagenetic calcite $\delta^{18}O$ and $\delta^{13}C$ values = black stars. $\delta^{18}O$ of inorganic calcite = 0.85‰ from *Cibicidoides havanensis* assumed to precipitate in isotopic equilibrium at the seafloor. The $\delta^{13}C$ of inorganic calcite is calculated by averaging the $\delta^{13}C$ values of surface dwelling taxa at TDP Site 18.

Site 18 (~−2.5‰ in $\delta^{18}O$; Fig. 3c and d and Table 1). However, as previously noted in Pearson (2012) this inter-site difference is least pronounced amongst the globigerinathekids and in *S. senni* (<2.0‰) suggesting that these thick-walled species preserve a signal closer to primary values than other planktic foraminiferal taxa (e.g. they are closest to the 1:1 line in Fig. 3d). In contrast, $\delta^{13}C$ offsets between glassy and recrystallized examples of any given species are typically much smaller ($\delta^{13}C$ values are closer to the 1:1 line in Fig. 3e) and more variable with surface dwelling taxa typically having $\delta^{13}C$ offsets ~±0.3‰, intermediate taxa ~+0.4‰ and the deepest dwelling planktic foraminifera giving the most pronounced offsets ~+0.8‰ (Table 1; Fig. 3e). This differential specific response results in a ~50% reduction in the surface-thermocline isotopic gradient for $\delta^{13}C$ at ODP Site 865 relative to TDP Site 18 implying compression of inter-species isotopic offsets (Fig. 3c) whereas there is relatively little change in $\delta^{18}O$ gradients between planktic species (Table 1).

3.2.2. Trace element/calcium ratios in foraminiferal calcite

Planktic foraminiferal Sr/Ca ratios generated in the same samples as the stable isotope measurements tend to be marginally higher in the intermediate and deeper dwelling species than in the surface dwellers at both sites (Fig. 4a and b; Table 2). B/Ca ratios have a more pronounced water column gradient with the highest ratios amongst known surface dwelling taxa and lowest in intermediate and deeper dwelling planktic foraminifera (Fig. 4d and e; Table 2). Benthic foraminifera at both sites are relatively enriched in [B] relative to their planktic counterparts, consistent with previous work (Table 2 only, not shown in Fig. 4; e.g., Rae et al., 2011). Comparison of trace element/calcium ratios between glassy and frosty planktic foraminiferal samples indicates that recrystallized specimens consistently have Sr/Ca and B/Ca ratios up to 40% lower than their glassy counterparts (Table 2; Fig. 4c and f). However, as with $\delta^{18}O$ and $\delta^{13}C$ values, Sr/Ca offsets are smallest in *G. euganea* and *S. senni* (e.g. closest to the 1:1 line in Fig. 4c) between the two sites but this remains

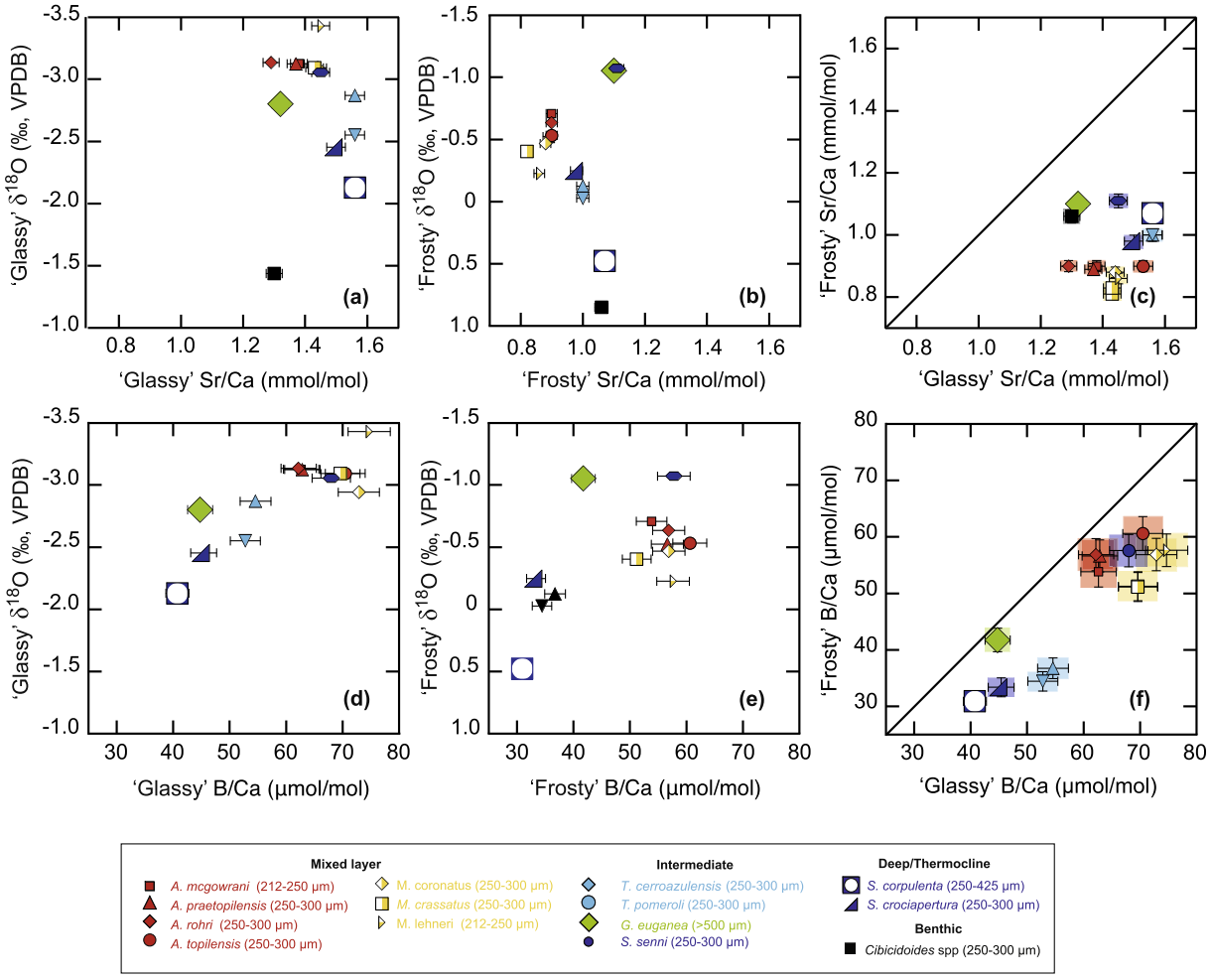

Fig. 4. Multi-species trace element/Ca ratios vs. $\delta^{18}O$ between glassy and recrystallized foraminiferal samples from TDP Site 18 (a and d) and ODP Site 865 (b and e), respectively. (c) and (f) Multi-species cross-plot of Sr/Ca and B/Ca ratios between glassy and frosty samples, respectively. Black diagonal line is the 1:1 relationship.

true only for *G. euganea* B/Ca ratios (Table 2). There are also no apparent large changes in the B/Ca or Sr/Ca gradient between surface and thermocline waters at the two sites.

3.2.3. Foraminiferal $\delta^{11}B$ in foraminiferal calcite

Measured $\delta^{11}B$ values at our study sites decrease from ~15.5‰ in the surface dwelling *Morozovelloides* and *Acarinina* to ~12.5‰ in thermocline dwelling and benthic species (Fig. 5 and Table 3). This is consistent with the calculated pattern of change in the $\delta^{11}B$ of the $B(OH)_4^-$ in the modern water column (but not in absolute values, compare Figs. 5 and 8a). At each of the sites the relative depth habitat of foraminifera species from $\delta^{11}B$-depth ranking is similar to those reconstructed using $\delta^{18}O$ and $\delta^{13}C$ values (Fig. 3 vs. 5) and inter-specific offsets are similar at each of the sites. However, *G. euganea* and *S. senni* at ODP Site 865 both record lower $\delta^{11}B$ values than predicted from their $\delta^{18}O$ values alone and are more in-keeping with the other surface dwelling taxa (*Morozovelloides* and *Acarinina*) (Fig. 3b vs. 5b). Crucially, comparison of $\delta^{11}B$ in the same species (and size fraction wherever possible; Table 3) with frosty and glassy taphonomies reveals little apparent offset outside of the calculated analytical uncertainty on the measurements such that no consistent patterns emerge between taxa at the two sites (Fig. 5c). The one

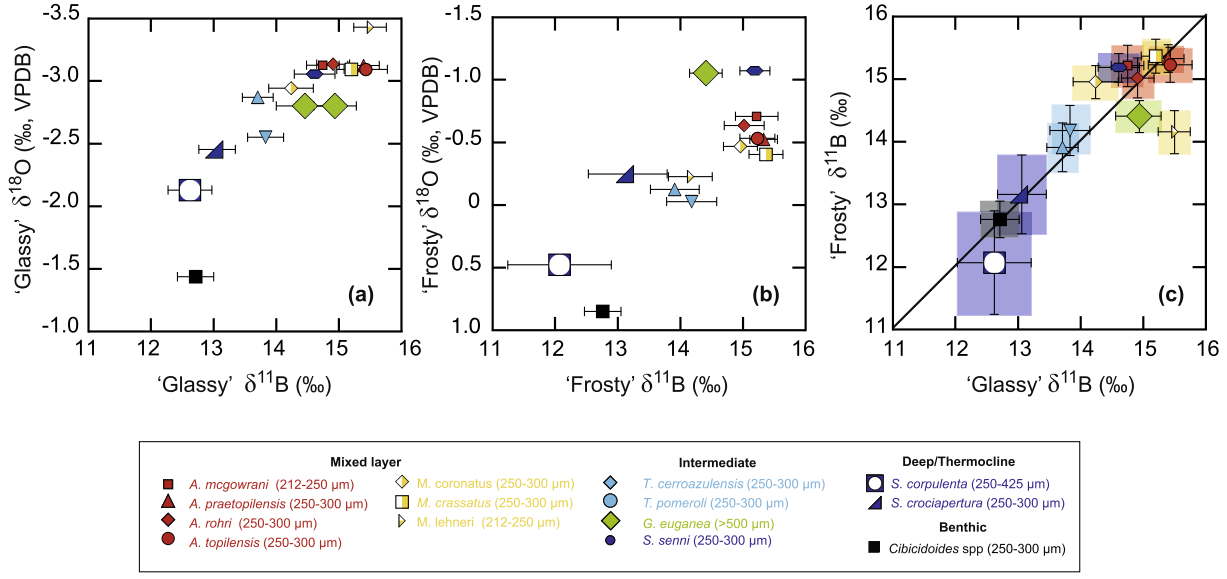

Fig. 5. Middle Eocene multi-species $\delta^{11}B$ arrays for glassy (a) and frosty (b) foraminiferal samples from TDP Site 18 and ODP Site 865, respectively and cross-plot of the two records (c). Black diagonal line in (c) is the 1:1 relationship. Error bars are external reproducibility of repeat analyses of Japanese Geological Survey *Porites* coral standard.

Table 3
$\delta^{11}B$ values for glassy and frosty foraminifera from TDP Site 18 and ODP Site 865, respectively.

Species	Sieve size fraction (µm)	TDP Site 18 $\delta^{11}B$ (‰)	2σ (‰)	ODP Site 865 $\delta^{11}B$ (‰)	2σ (‰)
Morozovelloides coronatus	250–300	14.24	0.36	14.96	0.27
Morozovelloides crassatus	250–300	15.20	0.23	15.35	0.26
Morozovelloides crassatus	250–300	–	–	15.38	0.27
Morozovelloides lehneri	212–250	15.50	0.26	14.16	0.35
Acarinina mcgowrani	212–250	14.75	0.26	15.22	0.34
Acarinina praetopilensis	250–300	15.40	0.25	15.33	0.22
Acarinina rohri	250–300	14.91	0.26	15.02	0.32
Acarinina topilensis	250–300	15.43	0.35	15.23	0.28
Subbotina senni	250–300	14.61	0.33	15.19	0.24
Globigerinatheka euganea	>500	14.94	0.34	14.41	0.26
Globigerinatheka euganea	>500	14.46	0.46	–	–
Turborotalia cerroazulensis	250–300	13.71	0.25	13.91	0.39
Turborotalia pomeroli	250–300	13.83	0.29	14.18	0.40
Subbotina corpulenta	355–425	12.62	0.35	–	–
Subbotina corpulenta	250–425	–	–	12.07	0.83
Subbotina crociapertura	300–355	13.06	0.29	13.16	0.63
Cibicidoides sp.	250–300	12.71	0.28	–	–
Cibicidoides havanensis	355–425	–	–	12.76	0.29

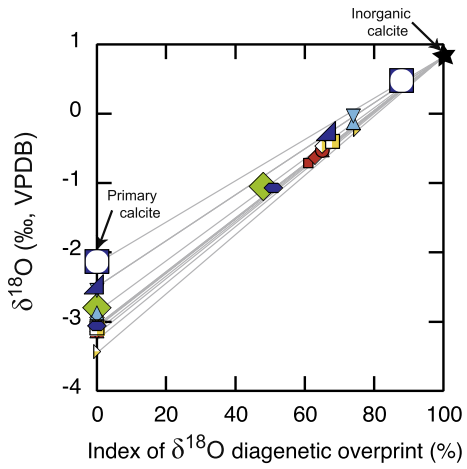

Fig. 6. Calculated Index of $\delta^{18}O$ diagenetic overprint for recrystallized planktic foraminiferal $\delta^{18}O$ values showing contribution of inorganic calcite (precipitated at the seafloor) to frosty foraminiferal test chemistry. Symbols as defined in Fig. 3.

exception is *M. lehneri* at ODP Site 865, which has a lower $\delta^{11}B$ value (>1‰) than reported at TDP Site 18.

3.2.4. Quantifying the composition and contribution of inorganic calcite to foraminiferal test chemistry

We calculate a >50% contribution of inorganic calcite to the chemical signature of foraminiferal tests at ODP Site 865 with the smallest estimated values recorded in *G. euganea* and *S. senni* (Fig. 6). Utilising the species-specific Index of $\delta^{18}O$ diagenetic overprint and Eq. (3), we estimate the B/Ca ratio of inorganic calcite as <56 μmol/mol, ~20 μmol/mol lower than primary (glassy) foraminiferal values (Table 2). From Eq. (4) we calculate the $\delta^{11}B$ of inorganic calcite, species-specific estimates range from 12‰ to 16‰ typically falling within the uncertainty of the $\delta^{11}B$ of their glassy counterparts.

We tested the sensitivity of our findings to the $\delta^{18}O$ of inorganic calcite ($\delta^{18}O_I$) employed and found that it had little impact on our overall conclusions. This is because the relative ordering of the degree of geochemical alteration of taxa remains the same so the impact on absolute values is relatively minor. For instance, if $\delta^{18}O_I$ was much higher than indicated by benthic foraminiferal $\delta^{18}O$ values (~2.0‰ vs. 0.85‰; e.g., reflecting the $\delta^{18}O$ offset between seawater and pore fluids at ODP Site 865 today; Paull et al. (1995)), then the Index of $\delta^{18}O$ diagenetic overprint values are >35%, B/Ca_I ratios remain <52 μmol/mol and $\delta^{11}B_I$ values range from 12‰ to 17‰.

4. DISCUSSION

4.1. The impact of diagenesis on planktic foraminiferal test $\delta^{13}C$ and $\delta^{18}O$ values

Taken at face value the large offset in $\delta^{18}O$ values (~2.5‰) implies ~12 °C offset in sea surface temperatures between the two study sites (Table 1). This large offset is inconsistent with the comparable oceanographic settings (and temperatures) of the two sites in the modern ocean (Locarnini et al., 2010) and inferred from Eocene GCM simulations (Huber and Caballero, 2011; Tindall et al., 2010). The most reasonable explanation for the large inter-site $\delta^{18}O$ offsets is the diagenetic recrystallization of planktic foraminiferal test calcite in cooler waters at the seafloor as previously predicted by theoretical and numerical modelling, *in-situ* secondary ion mass spectrometry of tests and diagenetic crystallites, and SEM observations (Kozdon et al., 2011; Pearson et al., 2001; Schrag et al., 1995; Sexton et al., 2006a). Indeed $\delta^{18}O$ values do converge towards the estimated $\delta^{18}O$ of inorganic calcite (see black star in Fig. 3c). Thus, the offset in $\delta^{18}O$ values is likely an artefact of this process and results in an underestimate of ~12 °C in sea surface temperatures calculated from recrystallized foraminifera (Table 1), consistent with the magnitude previously reported (Kozdon et al., 2011; Pearson et al., 2001; Sexton et al., 2006a). This interpretation is supported by our SEM observations (Fig. 2), which indicate that individual foraminifera tests from ODP Site 865 are completely recrystallized – no evidence of the original microgranular texture remains (Fig. 2j–r). Support is also given by the trace element/Ca ratio (see Sections 4.2 and 4.3) variations observed at the two study sites.

One explanation for the relatively small $\delta^{18}O$ offset between glassy and frosty samples in *G. euganea* and *S. senni* (Table 1) is that these taxa have thicker test walls than other taxa. There is no textural evidence that non-recrystallized areas may survive within the test wall (cf. Kozdon et al., 2011), because blocky recrystallization appears pervasive; however internal areas may have chemically exchanged less freely with external areas during the recrystallization process. This may also explain why *G. euganea* and *S. senni* record the lowest $\delta^{18}O$ values (warmest temperatures therefore the shallowest inferred water depth) in the whole foraminiferal assemblage at ODP Site 865 (Fig. 3b; see also Pearson, 2012).

In contrast to $\delta^{18}O$, $\delta^{13}C$ offsets between the two sites are more modest and within the range of natural surface water variability (~0.5‰) between the sites today (Tagliabue and Bopp, 2008). However, here we assume that biogenic carbonate precipitated under similar initial conditions. The $\delta^{13}C$ of diagenetic calcite is more similar to bulk carbonate values (black star in Fig. 3e) than bottom water values (Table 1), in these high carbonate, low organic matter sediments. Indeed planktic foraminiferal $\delta^{13}C$ values do converge towards a bulk carbonate value, which records an upper water column signal because it is predominantly comprised of planktic foraminifera and calcareous nannofossils (Berger et al., 1978). This scenario helps to reconcile the variable inter-specific $\delta^{13}C$ offsets in diagenetically altered foraminifera. For instance, the subbotinids, which have a biogenic $\delta^{13}C$ signature with the largest offset from diagenetic (inorganic) calcite, are most strongly impacted by diagenetic alteration (Table 1; Fig. 3d). In comparison, surface dwelling taxa typically show a much smaller and more variable shift in composition presumably because of the smaller difference between the $\delta^{13}C$ of diagenetic calcite and parent seawater (see also Pearson, 2012; Pearson et al., 2001). The variable response of $\delta^{13}C$ in the surface dwellers

may reflect some combination of dissolution (shifting test chemistry to lower $\delta^{13}C$ values), a function of inter-specific dissolution susceptibility, and the spread of primary $\delta^{13}C$ values as a function of ontogeny. Therefore, $\delta^{13}C$ is a less sensitive parameter to quantify diagenetic alteration than $\delta^{18}O$ because of additional uncertainties relating to estimating the $\delta^{13}C$ composition of diagenetic calcite.

In comparison to the obvious diagenetic offset on calculated sea surface temperatures using $\delta^{18}O$, little change is observed in the surface-thermocline water column temperature gradient in recrystallized calcite compared to that from well-preserved fossil calcite (Table 1). Compression of the $\delta^{13}C$ gradient is however more pronounced and creates the appearance of a more gradual transition in $\delta^{13}C$ values with increasing water depth (as also noted by John et al., 2013). The impacts of this are difficult to quantify but could bias both spatial and temporal reconstructions of relative changes in export production and/or nutrient utilisation in the photic zone.

4.2. Planktic foraminiferal Sr/Ca sensitivity to diagenetic alteration

The effect of dissolution and subsequent recrystallization on foraminiferal test chemistry is elegantly demonstrated by *in situ* analyses which reveal that inorganic crystallites in diagenetically altered foraminifera have Sr/Ca ratios two to three times lower than in the associated foraminiferal calcite (Kozdon et al., 2013; Regenberg et al., 2007). Our new results confirm this, with the Sr/Ca ratios of frosty planktic foraminiferal tests from ODP Site 865 ~33% lower than their glassy counterparts (Fig. 4c and Table 2). Notably the smallest change in Sr/Ca ratios (<25%) occurs in *G. euganea* and *S. senni*, which have a thick calcite crust.

This pattern is easily explained because Sr^{2+} is released from marine carbonates into pore fluids during calcite dissolution in the sediment column and then excluded during subsequent inorganic calcite precipitation from the same pore fluids (Baker et al., 1982; Gieskes et al., 1975; Richter and Liang, 1993). This leads to progressively lower $[Sr^{2+}]$ and Sr/Ca ratios in marine carbonates with increasing diagenetic alteration. Thus, diagenesis can result in distinctive down-core profiles of Sr/Ca and $[Sr^{2+}]$ of sediment pore fluids that can constrain the early diagenetic history of shallowly buried (<200 m) Neogene marine carbonates (see open circles in Fig. 7a; Baker et al., 1982; Matter et al., 1975). Many Neogene sediment pore fluid profiles show a pronounced increase in $[Sr^{2+}]$, from seawater values at the sediment–water interface to a maximum at ~200 m (see open symbols in Fig. 7a) inferred to represent the zone of maximum carbonate recrystallization (i.e., $[Sr^{2+}]$ exchange by carbonate dissolution and re-precipitation) (Baker et al., 1982). In these profiles, between ~200 m and the basement, $[Sr^{2+}]$ is invariant reflecting equilibrium between pore fluids and sediments. Thus, below ~200 m these records are not useful for constraining the diagenetic history of carbonate sediments (Baker et al., 1982; Richter and Liang, 1993; Rudnicki et al., 2001).

In contrast to the profiles observed in Neogene deep-sea sediments, the Sr/Ca pore fluid profile at ODP Site 865 shows little change in ratio with increasing sediment burial depth (see solid circles in Fig. 7). This vertical pore fluid profile is characteristic of the shallowly buried Paleogene deep-ocean sediments that are routinely targeted for paleoceanographic analyses, e.g., compare the almost identical downcore Sr/Ca profile of Sites U1334 and 865 in Fig. 7 (Edgar et al., 2013b; Rudnicki et al., 2001). This profile arises because of the absence of a thick pile of 'young' (<20 Ma), reactive sediments overlying Paleogene

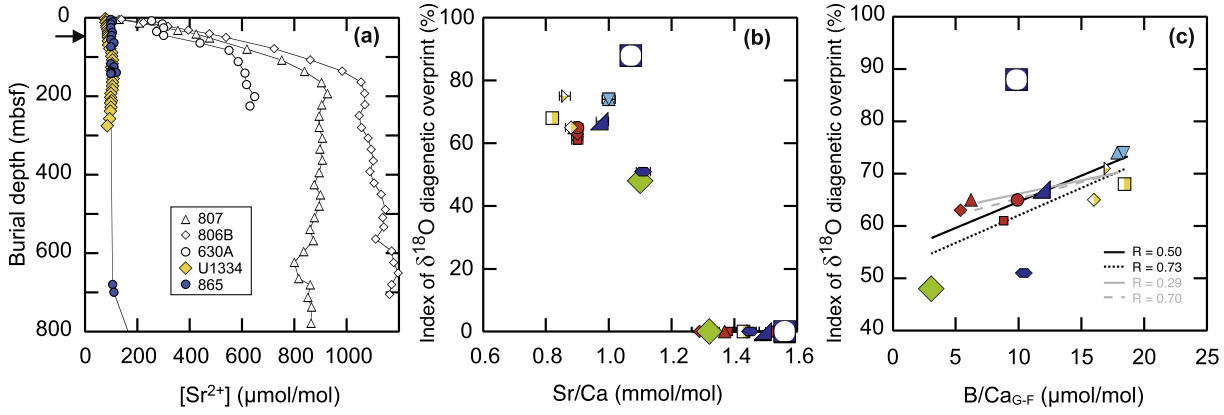

Fig. 7. (a) Contrasting $[Sr^{2+}]$ of sediment pore fluids between ODP Holes 806B and 807A (Shipboard Scientific Party, 1991) and 630A (Swart and Guzikowski, 1988) containing thick (>300 m) overburden of Neogene sediments above Paleogene deposits and those with shallowly-buried (>300 m) Paleogene sediments at ODP Site 865 (Shipboard Scientific Party, 1993) and IODP Site U1334 (Expedition 320/321 Scientists, 2010). Arrow indicates sample burial depth. Cross-plots in (b) and (c) show the relationship between our calculated Index of $\delta^{18}O$ diagenetic overprint (Section 4.1 and Fig. 6) – an estimate of how much geochemical alteration samples have undergone with (b) planktic foraminiferal Sr/Ca and (c) B/Ca offsets between glassy and frosty planktic foraminiferal species (Table 2) that may indicate diagenetic alteration of test chemistry. Correlation coefficients are shown with all samples included (solid black line), without *S. corpulenta* (dashed black line), without *G. euganea* (solid grey line) and without *S. corpulenta*, *G. euganea* and *S. senni* (dashed grey line) to highlight positive trend. Symbols as defined in Fig. 3.

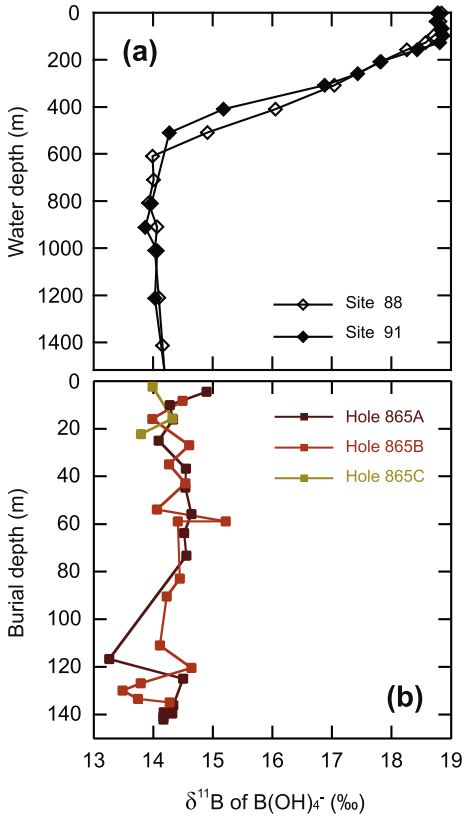

Fig. 8. Reconstructed $\delta^{11}B$ of $B(OH)_4^-$ in the water column (a) and in sediment pore fluids (b) at ODP Site 865 to constrain the $\delta^{11}B$ value of inorganic calcite. Profiles indicate similar sediment pore fluid and modern bottom water values.

sediments at ODP Site 865 so there is little exchange of Sr^{2+} in the sediment column at the present day (Richter and Liang, 1993). Sr^{2+} exchange still occurs between pore fluids and ocean crust but any chemical gradients are quickly lost by upward diffusion through the sediment column. Therefore unfortunately, this flattened profile provides little information on either the timing and/or location of carbonate alteration at this site in the past or present except to highlight that significant carbonate diagenesis is not occurring today consistent with decreasing sediment reactivity with sediment age (Richter and Liang, 1993). However, the large size and well-developed crystal faces on diagenetic carbonate crystallites in Early Paleogene sediments at ODP Site 865 suggest that diagenesis occurred early in the burial history of these sediments (<100 kyrs) before significant burial compaction occurred (Kozdon et al., 2013).

Given the obvious reduction in test Sr/Ca ratios as a function of diagenetic alteration it has been suggested (Bralower et al., 1997; Kozdon et al., 2013; Regenberg et al., 2007) that the Sr/Ca of foraminiferal calcite can be used to distinguish between altered and un-altered specimens. Ancient calcite is considered 'unaltered' if Sr/Ca ratios are >0.9 mmol/mol in the Holocene (Regenberg et al., 2007) or >1.2 mmol/mol in the Cretaceous (Bralower et al., 1997). However, any Sr/Ca cut-off will vary as a function of both the time interval and taxa being investigated. Here we plot our new Sr/Ca ratios against the Index of $\delta^{18}O$ diagenetic overprint for each species to try to place more quantitative constraints on diagenetic alteration (Fig. 7b). We find a correlation between the two variables and note that all altered specimens have Sr/Ca ratios of <1.2 mmol/mol. However, given the spread in the data, it appears unlikely, except in direct comparisons of time-equivalent samples from different sites that Sr/Ca ratios will be a valuable tool for quantitatively assessing the amount of diagenetic alteration a sample has undergone.

4.3. How robust are planktic foraminiferal test B/Ca ratios to diagenesis?

B/Ca ratios are consistently lower in recrystallized than in glassy foraminifera (by ~6% to 35%; Table 2). However, the controls on planktic foraminiferal B/Ca ratios in biogenic calcite are still poorly constrained and in the modern ocean can vary by ~10 μmol/mol between similar sites (Foster, 2008; Ni et al., 2007). If we assume that the B/Ca of biogenic calcite precipitated in surface waters was similar at the two study sites then the positive (albeit weak) correlation between those taxa with the highest Index of $\delta^{18}O$ diagenetic overprint and the largest B/Ca offsets between glassy and frosty taxa may support a diagenetic rather than primary origin for the offsets (Fig. 7c). Certainly published studies show decreasing B/Ca ratios with increasing water depth implying that B/Ca ratios are susceptible to depth dependent dissolution of a similar or lower magnitude to the offsets observed here, albeit over a much larger (and deeper) range of water depths than exists between our two sites (Coadic et al., 2013; Ni et al., 2007; Seki et al., 2010; Yu et al., 2007b). Recrystallized individuals at ODP Site 865 do show evidence of dissolution in the form of etching of the outer test surface, delamination and/or replacement of the test wall, and lower average test weights than in glassy foraminifera. Thus, dissolution and/or subsequent replacement of biogenic calcite with inorganic calcite at the seafloor and in the sediment column may modify test B/Ca ratios with implications for resulting paleoenvironmental reconstructions. However, further work is necessary to confidently discern the full impact of diagenesis on fossil test B/Ca ratios.

An understanding of the B/Ca of inorganic calcite precipitated from sediment pore fluids is essential to constraining the impact of diagenesis on fossil test B/Ca ratios. The B content of calcite is thought to be a function of the partition coefficient (K_D) of B between solid and liquid phases and the $B(OH)_4^-$ to HCO_3^- ratio of the precipitating medium which is pH-dependent ($K_D = [B/Ca]_{calcite}/[B(OH)_4^-/HCO_3^-]_{solution}$) (Hemming and Hanson, 1992; Yu et al., 2007b; Zeebe and Wolf-Gladrow, 2001). There is also an apparent pH dependency to the value of K_D itself, in addition to the pH dependency of $B(OH)_4^-$:HCO_3^- (e.g., Allen and Hönisch, 2012). Early empirical studies indicated that at pH values >8.5 K_D was typically higher for inorganic than for foraminiferal calcite (Sanyal et al., 1996, 2000; Zeebe et al., 2001). Thus, at pH values above ~8.5 inorganic calcite should contain more B than foraminiferal

calcite and vice versa at pH values <8.5. However, more recent foraminiferal studies (core-top and culture experiments) from a number of different planktic foraminiferal species yield K_D values that are more similar to, or higher (0.61×10^{-3}–1.79×10^{-3}) than, inorganic calcite at similar pH values to the original inorganic calcite precipitation experiments (Allen et al., 2011, 2012; Foster, 2008; Ni et al., 2007; Sanyal et al., 1996, 2000; Yu et al., 2007b). Thus, these new data suggest that the B/Ca ratio of inorganic calcite may be more similar to, or lower than, foraminiferal calcite, particularly when the lower pH of pore water and deep waters is considered (Rae et al., 2011; Spivack and You, 1997). This is consistent with calculations in Section 3.2.4, which suggests that the B/Ca ratio of inorganic calcite is likely to be lower than in biogenic calcite (<56 μmol/mol), which if correct, implies that B is preferentially lost and/or subsequently excluded during diagenesis. However it should be noted that considerable uncertainty remains as to the importance of factors other than pH (and the $B(OH)_4^-$:HCO_3^- ratio) in determining the B content of calcite, including (but not limited to) the rate of precipitation (Gabitov et al., 2014; Mavromatis et al., 2015; Ni et al., 2007), temperature (Foster, 2008; Tripati et al., 2009; Yu et al., 2007b), salinity (Allen et al., 2011) and light intensity (Babila et al., 2014). Indeed the concept of K_D as defined here (following Hemming and Hanson, 1992) may itself be at least partly incorrect (see Allen and Hönisch, 2012; Henehan et al., 2015).

4.4. Diagenetic impacts on planktic foraminiferal $\delta^{11}B$ records?

In contrast to $\delta^{18}O$, $\delta^{13}C$, Sr/Ca and perhaps B/Ca, the $\delta^{11}B$ of foraminifera analysed here are not obviously impacted by digenesis and the same $\delta^{11}B$-depth profile is observed at both sites (compare measurements to 1:1 line in Fig. 5c). This raises the following questions: (1) Why does recrystallization/diagenesis impact Sr/Ca, $\delta^{18}O$, $\delta^{13}C$ and possibly B/Ca but not, apparently, $\delta^{11}B$? and (2) are there any scenarios under which we might expect to observe a large diagenetic impact on the boron isotope composition of a foraminiferal test?

The $\delta^{11}B$ of *G. sacculifer* may be modified by partial dissolution (Hönisch and Hemming, 2004; Ni et al., 2007) with recent estimates showing that the $\delta^{11}B$ of *G. sacculifer* was lowered by ~0.7‰ when bottom waters become under-saturated with respect to carbonate ion (Seki et al., 2010). In contrast, there is little evidence for a partial dissolution effect on the $\delta^{11}B$ of *G. ruber* (Henehan et al., 2013; Ni et al., 2007; Seki et al., 2010). One hypothesis to explain this discrepancy is that the preferential dissolution of ontogenetic calcite from the test may shift the $\delta^{11}B$ of *G. sacculifer* towards the lower $\delta^{11}B$ of gametogenic calcite (precipitated in deeper waters) compared to *G. ruber*, which possesses little if any gametogenic calcite. However, [B] is heterogeneously distributed in foraminiferal tests and the divide between the different types of calcite is not clear-cut (Allen et al., 2011; Hathorne et al., 2009). Thus, the preferential removal of certain calcite layers with distinct chemical compositions within the test by dissolution is likely an overly simplistic hypothesis as highlighted by studies of other proxy systems (e.g., Hönisch and Hemming, 2004; Nürnberg et al., 1996). Regardless, dissolution of samples from ODP Site 865 does not appear to have lead to any significant modification of planktic foraminiferal $\delta^{11}B$ values.

The $\delta^{11}B$ of diagenetic calcite is a function of the pH and isotopic composition of the pore fluids from which it precipitates. The $\delta^{11}B$ (and the [B]) of pore fluids are in turn the product of a number of parameters and processes including temperature, pH, decomposition of organic matter, silica diagenesis, desorption of boron from and onto clays, chemical exchange with seafloor basalt and dissolution of carbonates (Ishikawa and Nakamura, 1993; Palmer et al., 1987; Rae et al., 2011; Spivack and Edmond, 1987; Spivack and You, 1997; Vengosh et al., 1991; Zeebe and Wolf-Gladrow, 2001). Therefore the relative impact of these processes on pore fluid $\delta^{11}B$ and thus, the $\delta^{11}B$ of $B(OH)_4^-$ incorporated into diagenetic calcite may be strongly site-specific (Brumsack and Zuleger, 1992; Ishikawa and Nakamura, 1993; Spivack and You, 1997; Spivack et al., 1993). The cumulative outcome of calcite and opal dissolution, oxidation of organic matter and desorption of B from clays in the sediment column should lead to lower pH and $\delta^{11}B$ values in pore fluids (Rae et al., 2011; Spivack and You, 1997; Zeebe and Wolf-Gladrow, 2001). Thus, inorganic calcite precipitated from these low pH and $\delta^{11}B$ fluids will also have a lower $\delta^{11}B$ than biogenic calcite precipitated in the water column. Indeed this interpretation is supported by Spivack and You (1997) who observed very low $\delta^{11}B$ values (~−5.5‰) in bulk carbonate at carbonate-rich site ODP Site 851. Unfortunately few $\delta^{11}B$ sediment pore-fluid studies exist, with which to constrain the $\delta^{11}B$ of inorganic calcite, for carbonate-rich deep-sea sections that are typical of those selected for paleoceanographic studies.

Seawater is able to mix rapidly (<10 kyrs; Paull et al. (1995)) through the highly permeable calcareous oozes, foraminiferal sands and limestones found at ODP Site 865, hindering the development of geochemical gradients within the pore fluids (as demonstrated by elemental profiles including Sr/Ca in Fig. 4a Shipboard Scientific Party (1993)). This is likely to have also been the case further back in time given the sites persistent position under an oligotrophic gyre and evidence of winnowing indicating high bottom water current flow at this site (Shipboard Scientific Party, 1993). Further, the high calcium carbonate content (>95%) of sediments and minor contributions of clay, silica, organic matter and other components reduces the possible contribution of boron from other sources to pore fluid chemistry (Shipboard Scientific Party, 1993).

Unfortunately [B] or $\delta^{11}B$ sediment pore fluid data were not measured at either of our study sites. Thus, to determine how the composition of inorganic calcite precipitated from pore fluids may vary down-core at ODP Site 865 we estimated the $\delta^{11}B$ of borate in pore fluid ($\delta^{11}B_{BOH_4\text{-pore fluid}}$) at the present day (Fig. 8b; Section 2.6). The resulting $\delta^{11}B_{BOH_4\text{-pore fluid}}$ profile shows little change with increasing burial depth and absolute values are equivalent to bottom waters at this site – in-keeping with the

invariant pH profile, strong seawater influence on pore fluid make-up and shallow sample burial (~39 m). Thus all else being equal, the $\delta^{11}B$ of calcite precipitated at the seafloor (i.e. benthic foraminifera) and from seawater-dominated pore fluids, should be similar.

4.5. Hypotheses for diagenetic alteration in foraminiferal tests

We propose three potential scenarios for how the diagenetic alteration of foraminiferal tests may occur and discuss the viability of each in light of our new dataset (with particular focus on the insights provided by our new $\delta^{11}B$ data).

(1) 'Open' system – if inorganic calcite precipitates from pore fluids in exchange with bottom waters, and thus with the same chemical composition and physical characteristics, then the $\delta^{11}B$ of inorganic calcite at ODP 865 will be equal to that of biogenic calcite precipitated from bottom waters. However, large pH offsets between the waters in which surface and deep-dwelling taxa precipitate their calcite (Fig. 5) means that surface dwelling taxa have biogenic calcite $\delta^{11}B$ values significantly higher than those at the seafloor (Table 3). Thus, their test calcite $\delta^{11}B$ will become progressively lower with increasing alteration. Given the degree of geochemical overprinting on foraminiferal test chemistry estimated from $\delta^{18}O$ values (Fig. 6), recrystallized surface dwelling taxa should have $\delta^{11}B$ values >1‰ lower than their glassy counterparts based on simple mixing calculations between two end-members (surface and bottom water $\delta^{11}B$ values; Eq. (4); Fig. 9). Carbonate dissolution (and other processes – see above) in the sediment column should lead to a further reduction in pore fluid $\delta^{11}B$ values exacerbating this offset. Such a large depletion in $\delta^{11}B$ values in surface dwelling frosty taxa is not observed (Fig. 5c). However, this situation could be mitigated if there was much less chemical alteration (<30%) than implied by the Index of $\delta^{18}O$ diagenetic overprint, but this necessitates a very high $\delta^{18}O$ of inorganic calcite (>6‰) or if our Index is not a sensitive quantifier of chemical alteration. For now it is difficult to reconcile precipitation of inorganic carbonate directly from bottom-water derived pore fluids with our observations.

(2) 'Closed' system – The best-case scenario for paleoceanographic studies is that diagenesis proceeds in a closed system, i.e., the foraminifera test dissolves and re-precipitates with no interaction with surrounding pore fluids. However, the observations that (1) planktic foraminiferal $\delta^{13}C$ and $\delta^{18}O$ values move towards a bulk sediment or seafloor end-member value and (2) strontium and boron may be lost with increasing alteration, imply that dissolution and recrystallization do not occur in a completely closed system (Figs. 4 and 7c). There must be at least some limited interaction or exchange with sediment pore fluids. Thus, while diagenesis may result in an overall loss of boron from the foraminiferal test there is surprisingly little or no accompanying isotopic fractionation of boron.

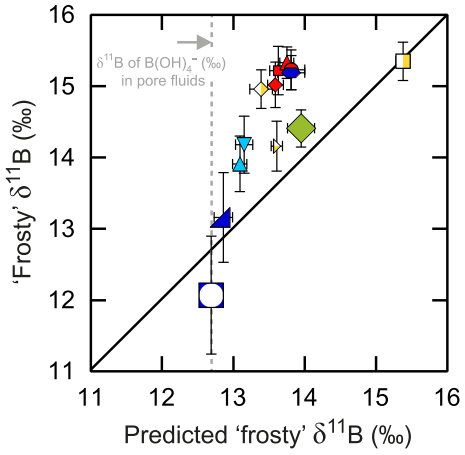

Fig. 9. Multi-species cross-plot of observed frosty $\delta^{11}B$ values from ODP Site 865 versus the predicted $\delta^{11}B$ values of frosty foraminiferal calcite if precipitation of diagenetic calcite proceeded in isotopic equilibrium with sediment pore fluids. Eq. (4) solved for $\delta^{11}B_F$ and $\delta^{11}B_I$ is 12.7‰ (Table 3) based on the assumption that epifaunal *Cibicidoides* sp. precipitates its test in isotopic equilibrium with bottom waters (Rae et al., 2011). Note that if the $\delta^{18}O$ of inorganic calcite is >0.85‰ the offset between predicted and observed values marginally decreases (offset is ~1‰ if $\delta^{18}O$ is 2‰) and if <0.85‰ it increases. Symbols as defined in Fig. 3.

(3) 'Partially open' system – Our dataset includes species living throughout the water column ($\delta^{11}B$ values span ~3‰; Fig. 5) thus, inorganic $\delta^{11}B$ values must be similar to 'primary' foraminiferal values to preserve interspecific offsets implying that the biogenic $\delta^{11}B$ signal is preserved in the recrystallized foraminifera studied here. Certainly our calculations (Section 3.2.4) of inorganic calcite B/Ca ratios are lower (<56 μmol/mol), but not much lower, than in biogenic calcite and $\delta^{11}B$ values of inorganic calcite are similar to 'primary' values recorded in equivalent glassy foraminifera. This supports previous studies (Pearson and Burgess, 2008; Pingitore, 1982) suggesting that foraminiferal recrystallization probably occurs within aqueous films at a very local scale within/immediately surrounding the foraminifer test (i.e., with only limited pore fluid exchange). Thus, foraminiferal calcite itself is likely the major source of the 'raw' chemical components utilised during recrystallization ensuring, in this case at least a near 100% preservation of original $\delta^{11}B$-signatures. This scenario is consistent with $\delta^{13}C$ and $\delta^{18}O$ values and Sr/Ca (and possibly B/Ca) ratios in foraminiferal calcite that while more sensitive to alteration than $\delta^{11}B$ (as shown by the larger offsets in absolute values between sites) largely preserve inter-specific offsets at each site despite the very different chemical compositions of inorganic calcite (particularly for $\delta^{18}O$).

Other factors that may help to reduce $\delta^{11}B$ offsets between biogenic and inorganic calcite are the reaction rates of recrystallization which are, as highlighted by numerical modelling, sediment pore fluid studies, bulk carbonate and foraminiferal studies, fastest in the first one million years after deposition and rapidly decrease with time (e.g., Fantle and DePaolo, 2006; Richter and Liang, 1993). Thus, early diagenesis typically proceeds rapidly after sediment deposition and thus, at relatively shallow burial depths (Edgar et al., 2013b; Richter and Liang, 1993; Rudnicki et al., 2001; Schrag et al., 1995). Therefore the $\delta^{11}B$ of pore fluids and environmental parameters should remain most similar to those the foraminifera originally precipitated from. Alternatively if inorganic calcite is subsequently demonstrated to have very low B/Ca ratios (<20 μmol/mol) as compared to biogenic foraminiferal calcite then regardless of its $\delta^{11}B$ value its contribution to test geochemistry will be very minor and there is a strong likelihood that some component of the original signal will still be preserved. However, in this situation a $\delta^{11}B$ of $B(OH)_4^-$ of pore fluids of >30‰ is necessary to ensure similar $\delta^{11}B$ values in glassy and frosty foraminiferal calcite.

Regardless of which scenario is correct, it is clear from the data presented here that the chemical and isotopic composition of recrystallized foraminifera is not simply the result of mixing primary biogenic and secondary pore-water derived diagenetic calcite. We hope that our dataset and these hypotheses will provide the impetus for future work to fully constrain the mechanism by which diagenesis occurs in foraminifera.

5. CAVEATS AND WAYS FORWARD

While our initial conclusions on the relative stability of $\delta^{11}B$ values in fossil foraminiferal calcite are promising for its use as a proxy, even in recrystallized foraminifera, caution is warranted before our findings are more widely extrapolated to different environments and other depositional settings where there may be additional controls on pore fluid compositions. For instance, if porewater $\delta^{11}B$ (and to a lesser extent pH, temperature and salinity) strongly vary from 'normal' seawater values as a function of processes on-going within the sediment, inorganic and biogenic calcite may have very different $\delta^{11}B$ values. Thus, even a small amount of diagenetic calcite will have a large impact on test $\delta^{11}B$. This will be particularly problematic if, unlike the situation at ODP 865, pore waters are closed to seawater preventing diffusion of pore fluid and promoting the development of strong geochemical gradients. The problem is also likely to be exacerbated as sediments are increasingly lithified with overgrowths becoming more extensive, eventually infilling specimens (Schlanger and Douglas, 1974). In these situations inorganic calcite typically precipitates deep in the sediment column where environmental parameters and the geochemistry of pore fluids are very different from those that the foraminifera originally precipitated in. However, such poorly preserved foraminifera are typically not utilised for geochemical analysis.

Future work should aim to test the robustness of our findings elsewhere by assessing foraminiferal $\delta^{11}B$ values across a wider range of taphonomies, time scales and sedimentary settings. In particular, the collection of $\delta^{11}B$ and [B] porewater profiles in seafloor sediments coupled with measurements of bulk and foraminiferal calcite from the same burial depths will be a valuable contribution to understanding diagenetic alteration of the boron system. Although perhaps the most direct method to identify the geochemical composition of diagenetic calcite is to utilise *in-situ* techniques such as Secondary Ionization Mass Spectrometry (SIMS) to compare the $\delta^{11}B$ of inorganic calcite overgrowths and primary foraminiferal calcite akin to work done on other paleoceanographically important proxies (Kasemann et al., 2009; Kozdon et al., 2013).

6. CONCLUSIONS

Here we utilise new geochemical data from two sites with inferred similar paleoceanographic settings but different carbonate fossil preservation states to assess the different sensitivities of elemental and stable isotope proxies to diagenetic alteration. Despite the influence of pervasive micron-scale diagenetic alteration on foraminiferal calcite observed by SEM we find that the relative depth stratification shown by $\delta^{18}O$ and $\delta^{13}C$ values in planktic foraminifera is generally well preserved. However, taxa with a thick calcite crust specifically the globigerinathekids and *S. senni* record a geochemical signal closest to original values. Foraminiferal Sr/Ca and B/Ca ratios are consistently lower in recrystallized compared to glassy tests suggesting susceptibility to post-mortem alteration, but further work is needed to more fully understand carbonate B/Ca ratios. In contrast, we show that the $\delta^{11}B$ values recorded in foraminiferal calcite (and inter-specific offsets) are not significantly impacted by extensive diagenetic alteration in shallowly buried samples (<50 m) from ODP Site 865. This may imply that recrystallization of foraminiferal calcite occurs in a relatively localized (and isolated) environment with the major contribution to diagenetic calcite geochemistry deriving from the dissolution of the foraminiferal test itself. Regardless of the exact mechanism our results potentially open the door to utilising the vast number of deep-sea sites hosting frosty foraminifera for reconstructing ocean pH in the past.

ACKNOWLEDGEMENTS

This research used samples provided by the Integrated Ocean Drilling Program (IODP). The authors would like to thank Sandra Nederbraght for technical assistance with $\delta^{18}O$ and $\delta^{13}C$ analyses, Marcus Badger for helpful discussions, and constructive comments from two anonymous reviewers and Associate Editor Yair Rosenthal. Financial support was provided in the form of a Natural Research Environment Council (NERC) Postdoctoral Research Fellowship (NE/H016457/1) and Leverhulme Early Career Fellowship (ECF-2013-608) to KME and NERC Grants awarded to PNP (NE/I005870/1) and GLF (NE/I005595/1).

REFERENCES

Allen K. A. and Hönisch B. (2012) The planktic foraminiferal B/Ca proxy for seawater carbonate chemistry: a critical evaluation. *Earth Planet. Sci. Lett.* **345**, 203–211.

Allen K. A., Hönisch B., Eggins S. M., Yu J., Spero H. J. and Elderfield H. (2011) Controls on boron incorporation in cultured tests of the planktic foraminifer *Orbulina universa*. *Earth Planet. Sci. Lett.* **309**, 291–301.

Allen K. A., Hönisch B., Eggins S. M. and Rosenthal Y. (2012) Environmental controls on B/Ca in calcite tests of the tropical planktic foraminifer species *Globigerinoides ruber* and *Globigerinoides sacculifer*. *Earth Planet. Sci. Lett.* **351**, 270–280.

Babila T. L., Rosenthal Y. and Conte M. H. (2014) Evaluation of the biogeochemical controls on B/Ca of *Globigerinoides ruber* white from the Oceanic Flux Program, Bermuda. *Earth Planet. Sci. Lett.* **404**, 67–76.

Badger M. P. S., Lear C. H., Pancost R. D., Foster G. L., Bailey T. R., Leng M. J. and Abels H. A. (2013) CO_2 drawdown following the middle Miocene expansion of the Antarctic Ice Sheet. *Paleoceanography*, 28.

Baker P. A., Gieskes J. M. and Elderfield H. (1982) Diagenesis of carbonates in deep-sea sediments; evidence from Sr/Ca ratios and interstitial dissolved Sr^{2+} data. *J. Sediment. Res.* **52**, 71–82.

Barker S., Greaves M. and Elderfield H. (2003) A study of cleaning procedures used for foraminiferal Mg/Ca paleothermometry. *Geochem. Geophys. Geosyst.* **4**.

Bé A. W., Morse J. and Harrison S. (1975) Progressive dissolution and ultrastructural breakdown of planktonic foraminifera. *Cushman Foundation Foraminiferal Res.* **13**, 27–55 (special publication).

Bemis B. E., Spero H. J., Bijma J. and Lea D. W. (1998) Reevaluation of the oxygen isotopic composition of planktonic foraminifera: experimental results and revised paleotemperature equations. *Paleoceanography* **13**, 150–160.

Berger W. H., Killingley J. S. and Vincent E. (1978) Stable isotopes in deep-sea carbonates: box core ERDC-92, West Equatorial Pacific. *Oceanol. Acta* **1**, 203–216.

Birch H., Coxall H. K., Pearson P. N., Kroon D. and O'Regan M. (2013) Planktonic foraminifera stable isotopes and water column structure: disentangling ecological signals. *Mar. Micropaleontol.* **101**, 127–145.

Blow W. H. (1979) *The Cainozoic Globigerinida*. E.J. Brill, Leiden.

Bown P. R., Dunkley Jones T., Lees J. A., Randell R. D., Mizzi J. A., Pearson P. N., Coxall H. K., Young J. R., Nicholas C. J., Karega A., Singano J. and Wade B. S. (2008) A Paleogene calcareous microfossil Konservat-Lagerstätte from the Kilwa Group of coastal Tanzania. *Geol. Soc. Am. Bull.* **120**, 3–12.

Bralower T. J., Zachos J. C., Thomas E., Parrow M., Paull C. K., Kelly D. C., Silva I. P., Sliter W. V. and Lohmann K. C. (1995) Late Paleocene to Eocene paleoceanography of the equatorial Pacific Ocean: stable isotopes recorded at Ocean Drilling Program Site 865, Allison Guyot. *Paleoceanography* **10**, 841–865.

Bralower T. J., Fullagar P. D., Paull C. K., Dwyer G. S. and Leckie R. M. (1997) Mid-Cretaceous strontium-isotope stratigraphy of deep-sea sections. *Geol. Soc. Am. Bull.* **109**, 1421–1442.

Brown S. J. and Elderfield H. (1996) Variations in Mg/Ca and Sr/Ca ratios of planktonic foraminifera caused by postdepositional dissolution: evidence of shallow Mg-dependent dissolution. *Paleoceanography* **11**, 543–551.

Brumsack H. J. and Zuleger E. (1992) Boron and boron isotopes in pore waters from ODP Leg 127, Sea of Japan. *Earth Planet. Sci. Lett.* **113**, 427–433.

Burgess C. E., Pearson P. N., Lear C. H., Morgans H. E. G., Handley L., Pancost R. D. and Schouten S. (2008) Middle Eocene climate cyclicity in the southern Pacific: implications for global ice volume. *Geology* **36**, 651–654.

Catanzaro E. J., Champion C. E., Garner E. L., Marinenko G., Sappenfield K. M. and Shields W. R. (1970) *Boric Assay; Isotopic, and Assay Standard Reference Materials*. National Bureau of Standards Special Publication, Washington, DC.

Coadic R., Bassinot F., Dissard D., Douville E., Greaves M. and Michel E. (2013) A core-top study of dissolution effect on B/Ca in *Globigerinoides sacculifer* from the tropical Atlantic: potential bias for paleo-reconstruction of seawater carbonate chemistry. *Geochem. Geophys. Geosyst.* **14**, 1053–1068.

Cramer B. S., Miller K. G., Barrett P. J. and Wright J. D. (2011) Late Cretaceous-Neogene trends in deep ocean temperature and continental ice volume: reconciling records of benthic foraminiferal geochemistry ($\delta^{18}O$ and Mg/Ca) with sea level history. *J. Geophys. Res.: Oceans* **116**, C12023.

D'Hondt S. and Arthur M. A. (1996) Late Cretaceous oceans and the cool tropic paradox. *Science* **271**, 1838–1841.

Edgar K. M., Bohaty S. M., Gibbs S. J., Sexton P. F., Norris R. D. and Wilson P. A. (2013a) Symbiont 'bleaching' in planktic foraminifera during the Middle Eocene Climatic Optimum. *Geology* **41**, 15–18.

Edgar K. M., Pälike H. and Wilson P. A. (2013b) Testing the impact of diagenesis on the $\delta^{18}O$ and $\delta^{13}C$ of benthic foraminiferal calcite from a sediment burial depth transect in the equatorial Pacific. *Paleoceanography* **28**, 468–480.

Emiliani C. (1954) Depth habitats of some species of pelagic Foraminifera as indicated by oxygen isotope ratios. *Am. J. Sci.* **252**, 149–158.

Expedition 320/321 Scientists (2010) Site U1334. In *Proceedings of the Integrated Ocean Drilling Program, 320/321* (eds. H. Pälike, M. Lyle, H. Nishi, I. Raffi, K. Gamage, A. Klaus and Expedition 320/321 Scientists). Integrated Ocean Drilling Program Management International, Inc., Tokyo.

Fairbanks R. G., Wiere P. H. and Be A. (1980) Vertical distribution and isotopic composition of living planktonic Foraminifera in the Western North Atlantic. *Science* **207**, 61–63.

Fantle M. S. and DePaolo D. J. (2006) Sr isotopes and pore fluid chemistry in carbonate sediment of the Ontong Java Plateau: calcite recrystallization rates and evidence for a rapid rise in seawater Mg over the last 10 million years. *Geochim. Cosmochim. Acta* **70**, 3883–3904.

Folk R. L. (1965) Some aspects of recrystallisation in ancient limestones. In *Dolomitization and Limestones Diagenesis* (eds. L. C. Pray and R. C. Murray). The Society of Economic Paleontologists and Mineralogists, pp. 14–48.

Foster G. L. (2008) Seawater pH, PCO_2 and CO_3^{2-} variations in the Caribbean Sea over the last 130 kyr: a boron isotope and B/Ca study of planktic Foraminifera. *Earth Planet. Sci. Lett.* **271**, 254–266.

Foster G. L., Pogge von Strandmann P. A. E. and Rae J. W. B. (2010) Boron and magnesium isotopic composition of seawater. *Geochem. Geophys. Geosyst.*, 11.

Foster G. L., Lear C. H. and Rae J. W. B. (2012) The evolution of pCO_2, ice volume and climate during the middle Miocene. *Earth Planet. Sci. Lett.* **341**, 243–254.

Gabitov R. I., Rollion-Bard C., Tripati A. and Sadekov A. (2014) In situ study of boron partitioning between calcite and fluid at different crystal growth rates. *Geochim. Cosmochim. Acta* **137**, 81–92.

Gieskes J. M., Kastner M. and Warner T. (1975) Evidence for extensive diagenesis, Madagascar Basin, Deep Sea Drilling Site 245. *Geochim. Cosmochim. Acta* **39**, 1385–1393.

Hathorne E. C., James R. H. and Lampitt R. S. (2009) Environmental versus biomineralization controls on the

intratest variation in the trace element composition of the planktonic foraminifera *G. inflata* and *G. scitula*. *Paleoceanography*, 24.

Hemleben C., Spindler M. and Anderson O. R. (1989) *Modern Planktonic Foraminifera*. Springer-Verlag, New York.

Hemming N. G. and Hanson G. N. (1992) Boron isotopic composition and concentration in modern marine carbonates. *Geochim. Cosmochim. Acta* **56**, 537–543.

Hemming N. G. and Hönisch B. (2007) Boron isotopes in marine carbonate sediments and the pH of the ocean. In *Proxies in Late Cenozoic Paleoceanography* (eds. C. Hillaire-Marcel and A. DeVernal), pp. 717–734.

Henehan M. J., Rae J. W. B., Foster G. L., Erez J., Prentice K. C., Kučera M., Bostock H. C., Martínez-Botí M. A., Milton J. A., Wilson P. A., Marshall B. J. and Elliott T. (2013) Calibration of the boron isotope proxy in the planktonic foraminifera *Globigerinoides ruber* for use in palaeo-CO_2 reconstruction. *Earth Planet. Sci. Lett.* **364**, 111–122.

Henehan M. J., Foster G. L., Rae J. W. B., Prentice K. C., Erez J., Bostock H. C., Marshall B. J. and Wilson P. A. (2015) Evaluating the utility of B/Ca ratios in planktic foraminifera as a proxy for the carbonate system: a case study of *Globigerinoides ruber*. *Geochem. Geophys. Geosyst.*, 1052–1059.

Hönisch B. and Hemming N. G. (2004) Ground-truthing the boron isotope-paleo-pH proxy in planktonic foraminifera shells: partial dissolution and shell size effects. *Paleoceanography*, 19.

Hönisch B., Hemming N. G., Archer D., Siddall M. and McManus J. F. (2009) Atmospheric carbon dioxide concentration across the mid-Pleistocene transition. *Science* **324**, 1551–1554.

Huber M. and Caballero R. (2011) The early Eocene equable climate problem revisited. *Clim. Past* **7**, 603–633.

Ishikawa T. and Nakamura E. (1993) Boron isotope systematics of marine sediments. *Earth Planet. Sci. Lett.* **117**, 567–580.

John E. H., Pearson P. N., Coxall H. K., Birch H., Wade B. S. and Foster G. L. (2013) Warm ocean processes and carbon cycling in the Eocene. *Philos. Trans. R. Soc. A*, 371.

Kasemann S. A., Schmidt D. N., Bijma J. and Foster G. L. (2009) In situ boron isotope analysis in marine carbonates and its application for foraminifera and palaeo-pH. *Chem. Geol.* **260**, 138–147.

Kim S. T. and O'Neil J. R. (1997) Equilibium and nonequilibrium oxygen isotope effects in synthetic carbonates. *Geochim. Cosmochim. Acta* **61**, 3461–3475.

Klochko K., Kaufman A. J., Yao W., Byrne R. H. and Tossell J. A. (2006) Experimental measurement of boron isotope fractionation in seawater. *Earth Planet. Sci. Lett.* **248**, 276–285.

Kozdon R., Kelly D. C., Kita N. T., Fournelle J. H. and Valley J. W. (2011) Planktonic foraminiferal oxygen isotope analysis by ion microprobe technique suggests warm tropical sea surface temperatures during the early paleogene. *Paleoceanography* **26**, PA3206.

Kozdon R., Kelly D. C., Kitajima K., Strickland A., Fournelle J. H. and Valley J. W. (2013) In situ $\delta^{18}O$ and Mg/Ca analyses of diagenetic and planktic foraminiferal calcite preserved in a deep-sea record of the Paleocene–Eocene Thermal Maximum. *Paleoceanography* **28**, 517–528.

Lea D. W. (2014) Elemental and isotopic proxies of past ocean temperatures. In *Treatise on Geochemistry, 2nd ed.* (eds. K. K. Turekian and H. D. Holland). Elsevier, Oxford, pp. 373–397.

Lea D. W., Mashiotta T. A. and Spero H. J. (1999) Controls on magnesium and strontium uptake in planktonic foraminifera determined by live culturing. *Geochim. Cosmochim. Acta* **63**, 2369–2379.

Locarnini R. A., Mishonov A. V., Antonov J. I., Boyer T. P., Garcia H. E., Baranova O. K., Zweng M. M. and Johnson D. R. (2010) *World ocean atlas 2009, Temperature* **vol 1**. U.S. Government Printing Office, Washington, DC.

Lohmann G. P. (1995) A model for variation in the chemistry of planktonic foraminifera due to secondary calcification and selective dissolution. *Paleoceanography* **10**, 445–457.

Matter A., Douglas R. G. and Perch-Nielsen K. (1975) Fossil preservation, geochemistry, and diagenesis of pelagic carbonates from Shatsky Rise, northwest Pacific. In *Initial Reports of the Deep Sea Drilling Project* (ed. J. V. Gardner). U.S. Gov. Print. Off., Washington, DC, pp. 891–907.

Mavromatis V., Montouillout V., Noireaux J., Gaillardet J. and Schott J. (2015) Characterization of boron incorporation and speciation in calcite and aragonite from co-precipitation experiments under controlled pH, temperature and precipitation rate. *Geochim. Cosmochim. Acta* **150**, 299–313.

Ni Y., Foster G. L., Bailey T., Elliott T., Schmidt D. N., Pearson P., Haley B. and Coath C. (2007) A core top assessment of proxies for the ocean carbonate system in surface-dwelling foraminifers. *Paleoceanography*, 22.

Nicholas C. J., Pearson P. N., Bown P. R., Dunkley Jones T., Huber B. T., Karega A., Lees J. A., McMillan I. K., O'Halloran A., Singano J. M. and Wade B. S. (2006) Stratigraphy and sedimentology of the upper cretaceous to Paleogene Kilwa Group, southern coastal Tanzania. *J. Afr. Earth Sc.* **45**, 431–466.

Norris R. D. and Wilson P. A. (1998) Low-latitude sea-surface temperatures for the mid-Cretaceous and the evolution of planktic foraminifera. *Geology* **26**, 823–826.

Nürnberg D., Bijma J. and Hemleben C. (1996) Assessing the reliability of magnesium in foraminiferal calcite as a proxy for water mass temperatures. *Geochim. Cosmochim. Acta* **60**, 803–814.

Palmer M. R., Spivack A. J. and Edmond J. M. (1987) Temperature and pH controls over isotopic fractionation during adsorption of boron on marine clay. *Geochim. Cosmochim. Acta* **51**, 2319–2323.

Palmer M. R., Pearson P. N. and Cobb S. J. (1998) Reconstructing past ocean pH-depth profiles. *Science* **282**, 1468–1471.

Paull C. K., Fullager P. D., Bralower T. J. and Rohl U. (1995) Seawater ventilation of mid-pacific guyots drilled during Leg 143. In *Proceedings of the Ocean Drilling Program, Scientific Results* (eds. E. L. Winterer, W. W. Sager, J. V. Firth and J. M. Sinton), pp. 231–241.

Pearson P. N. (2012) Oxygen isotopes in foraminifera: overview and historical review. In *Reconstructing Earth's Deep Time Climate – The State of the Art in 2012. The Paleontological Society Papers* (eds. L. C. Ivany and B. T. Huber), pp. 1–38.

Pearson P. N. and Burgess C. E. (2008) Foraminifer test preservation and diagenesis: comparison of high latitude Eocene sites. *Geol. Soc.* **303**, 59–72 (London, special publications).

Pearson P. N. and Palmer M. R. (1999) Middle Eocene seawater pH and atmospheric carbon dioxide concentrations. *Science* **284**, 1824–1826.

Pearson P. N. and Palmer M. R. (2000) Atmospheric carbon dioxide concentrations over the past 60 million years. *Nature* **406**, 695–699.

Pearson P. N., Shackleton N. J. and Hall M. A. (1993) Stable isotope paleoecology of middle Eocene planktonic foraminifera and multi-species isotope stratigraphy, DSDP Site 523, South Atlantic. *J. Foraminiferal Res.* **23**, 123–140.

Pearson P. N., Ditchfield P. W., Singano J., Harcourt-Brown K. G., Nicholas C. J., Olsson R. K., Shackleton N. J. and Hall M. A. (2001) Warm tropical sea surface temperatures

in the Late Cretaceous and Eocene epochs. *Nature* **413**, 481–487.

Pearson P. N., Olsson R. K., Huber B. T., Hemleben C., Berggren W. A. and Coxall H. K. (2006) Overview of Eocene planktonic foraminiferal taxonomy, paleoecology, phylogeny, and biostratigraphy. *Cushman Foundation for Foraminiferal Res.* **41**, 11–28 (special publication).

Pearson P. N., van Dongen B. E., Nicholas C. J., Pancost R. D., Schouten S., Singano J. M. and Wade B. S. (2007) Stable warm tropical climate through the Eocene Epoch. *Geology* **35**, 211–214.

Pearson P. N., Foster G. L. and Wade B. S. (2009) Atmospheric carbon dioxide through the Eocene–Oligocene climate transition. *Nature* **461**, 1110–U1204.

Pearson P. N., Evans S. L. and Evans J. (2015) Effect of diagenetic recrystallisation on the strength of planktonic foraminifer tests under compression. *J. Micropalaeontol.* **34**, 59–64.

Penman D. E., Hönisch B., Zeebe R. E., Thomas E. and Zachos J. C. (2014) Rapid and sustained surface ocean acidification during the Paleocene–Eocene Thermal Maximum. *Paleoceanography*, 2014PA002621.

Pingitore N. E. (1982) The role of diffusion during carbonate diagenesis. *J. Sediment. Petrol.* **52**, 27–39.

Rae J. W. B., Foster G. L., Schmidt D. N. and Elliott T. (2011) Boron isotopes and B/Ca in benthic foraminifera: proxies for the deep ocean carbonate system. *Earth Planet. Sci. Lett.* **302**, 403–413.

Regenberg M., Nürnberg D., Schönfeld J. and Reichart G. J. (2007) Early diagenetic overprint in Caribbean sediment cores and its effect on the geochemical composition of planktonic foraminifera. *Biogeosciences* **4**, 957–973.

Richter F. M. and Liang Y. (1993) The rate and consequences of Sr diagenesis in deep-sea carbonates. *Earth Planet. Sci. Lett.* **117**, 553–565.

Roden G. I., Fredericks W. J. and Experiment W. O. C. (1995) *Pacific Ocean WOCE P14N, CTD Data Report: R/V Thomas G. Thompson, 5 July–1 September 1993*. School of Oceanography, University of Washington.

Rudnicki M. D., Wilson P. A. and Anderson W. T. (2001) Numerical models of diagenesis, sediment properties, and pore fluid chemistry on a paleoceanographic transect: Blake Nose, Ocean Drilling Program Leg 171B. *Paleoceanography* **16**, 563–575.

Sager W. W., Winterer E. L. and Firth J. V., et al. (1993) *Proceedings of the Ocean Drilling Program, Initial Reports*. Ocean Drilling Program, College Station, TX.

Sanyal A., Hemming N. G., Broecker W. S., Lea D. W., Spero H. J. and Hanson G. N. (1996) Oceanic pH control on the boron isotopic composition of foraminifera: evidence from culture experiments. *Paleoceanography* **11**, 513–517.

Sanyal A., Nugent M., Reeder R. J. and Bijma J. (2000) Seawater pH control on the boron isotopic composition of calcite: evidence from inorganic calcite precipitation experiments. *Geochim. Cosmochim. Acta* **64**, 1551–1555.

Schlanger S. O. and Douglas R. G. (1974) The pelagic ooze-chalk-limestone transition and its implication for marine stratigraphy. In *Pelagic Sediments: on Land and under the Sea* (eds. K. J. Hsu and H. Jenkyns), pp. 117–148.

Schrag D. P., DePaolo D. J. and Richter F. M. (1995) Reconstructing past sea surface temperatures: correcting for diagenesis of bulk marine carbonate. *Geochim. Cosmochim. Acta* **59**, 2265–2278.

Seki O., Foster G. L., Schmidt D. N., Mackensen A., Kawamura K. and Pancost R. D. (2010) Alkenone and boron-based pliocene pCO_2 records. *Earth Planet. Sci. Lett.* **292**, 201–211.

Sexton P. E., Wilson P. A. and Pearson P. N. (2006a) Microstructural and geochemical perspectives on planktic foraminiferal preservation: "Glassy" versus "Frosty". *Geochem. Geophys. Geosyst.* **7**.

Sexton P. F., Wilson P. A. and Pearson P. N. (2006b) Palaeoecology of late middle Eocene planktic foraminifera and evolutionary implications. *Mar. Micropaleontol.* **60**, 1–16.

Shipboard Scientific Party (1991) Site 806. In *Proceedings of the Ocean Drilling Program, Initial Reports* (eds. L. W. Kroenke, W. H. Berger, T. R. Janecek and Shipboard Scientific Party). Ocean Drilling Program, College Station, TX, pp. 291–367.

Shipboard Scientific Party (1993) Site 865. In *Proceedings of the Ocean Drilling Program, Initial Reports 143* (eds. W. W. Sager, E. L. Winterer, J. V. Firth and S. S. Party). Ocean Drilling Program, College Station, TX, pp. 111–180.

Sorby H. C. (1879) Structure and origin of limestones. *Proc. Geol. Soc. Lond.* **35**, 56–95.

Spero H. and Williams D. F. (1988) Extracting environmental information from planktonic foraminiferal $\delta^{13}C$ data. *Nature* **335**, 717–719.

Spivack A. J. and Edmond J. M. (1987) Boron isotope exchange between seawater and the oceanic crust. *Geochim. Cosmochim. Acta* **51**, 1033–1043.

Spivack A. J. and You C. F. (1997) Boron isotopic geochemistry of carbonates and pore waters, Ocean Drilling Program Site 851. *Earth Planet. Sci. Lett.* **152**, 113–122.

Spivack A. J., You C. F. and Smith H. J. (1993) Foraminiferal boron isotope ratios as a proxy for surface ocean pH over the past 21-Myr. *Nature* **363**, 149–151.

Stoll H. M., Schrag D. P. and Clemens S. C. (1999) Are seawater Sr/Ca variations preserved in Quaternary foraminifera? *Geochim. Cosmochim. Acta* **63**, 3535–3547.

Swart P. K. and Guzikowski M. (1988) Interstitial-water chemistry and diagenesis of periplatform sediments from the Bahamas, ODP Leg 101. In *Proceedings of the Ocean Drilling Program, Scientific Results* (eds. J. A. Austin and W. Schlager). Ocean Drilling Program, College Station, Texas, pp. 363–380.

Tagliabue A. and Bopp L. (2008) Towards understanding global variability in ocean carbon-13. *Global Biogeochem. Cycles* **22**, GB1025.

Tindall J., Flecker R., Valdes P., Schmidt D. N., Markwick P. and Harris J. (2010) Modelling the oxygen isotope distribution of ancient seawater using a coupled ocean–atmosphere GCM: implications for reconstructing early Eocene climate. *Earth Planet. Sci. Lett.* **292**, 265–273.

Tripati A. K., Roberts C. D. and Eagle R. A. (2009) Coupling of CO_2 and ice sheet stability over major climate transitions of the last 20 million years. *Science* **326**, 1394–1397.

van Heuven S., Pierrot D., Rae J. W. B., Lewis E. and Wallace D. W. R. (2011) MATLAB program developed for CO_2 system calculations. In *Carbon Dioxide Information Analysis Center*. O.R.N.L., U.S., Department of Energy, O.R., Tennessee.

Vengosh A., Kolodny Y., Starinsky A., Chivas A. R. and McCulloch M. T. (1991) Coprecipitation and isotopic fractionation of boron in modern biogenic carbonates. *Geochim. Cosmochim. Acta* **55**, 2901–2910.

Wade B. S., Al-Sabouni N., Hemleben C. and Kroon D. (2008) Symbiont bleaching in fossil planktonic foraminifera. *Evol. Ecol.* **22**, 253–265.

Wade B. S., Pearson P. N., Berggren W. A. and Pälike H. (2011) Review and revision of Cenozoic tropical planktonic foraminiferal biostratigraphy and calibration to the geomagnetic polarity and astronomical time scale. *Earth Sci. Rev.* **104**, 111–142.

Wilson P. A. and Norris R. D. (2001) Warm tropical ocean surface and global anoxia during the mid-Cretaceous period. *Nature* **412**, 425–429.

Wilson P. A., Norris R. D. and Cooper M. J. (2002) Testing the Cretaceous greenhouse hypothesis using glassy foraminiferal calcite from the core of the Turonian tropics on Demerara Rise. *Geology* **30**, 607–610.

Yu J., Elderfield H., Greaves M. and Day J. (2007a) Preferential dissolution of benthic foraminiferal calcite during laboratory reductive cleaning. *Geochem. Geophys. Geosyst.* **8**, Q06016.

Yu J., Elderfield H. and Hönisch B. (2007b) B/Ca in planktonic foraminifera as a proxy for surface seawater pH. *Paleoceanography*, 22.

Zachos J. C., Stott L. D. and Lohmann K. C. (1994) Evolution of early Cenozoic marine temperatures. *Paleoceanography* **9**, 353–387.

Zeebe R. E. and Wolf-Gladrow D. A. (2001) Chapter 3: stable isotope fractionation. In *Elsevier Oceanography Series* (eds. E. Z. Richard and W.-G. Dieter). Elsevier, pp. 141–250.

Zeebe R. E., Sanyal A., Ortiz J. D. and Wolf-Gladrow D. A. (2001) A theoretical study of the kinetics of the boric acid-borate equilibrium in seawater. *Mar. Chem.* **73**, 113–124.

Associate editor: Yair Rosenthal